Formation of Interstitial Branches Selectively Within the Red Nucleus by Deep Cerebellar Nuclei–Derived Commissural Axons During Target Recognition

（発達期小脳核ニューロン軸索の正中交差後における
赤核認識に関する研究）

Satoshi Hara

Cellular and Molecular Neurobiology Laboratory,
Graduate School of Frontier Biosciences,
Osaka University

CONTENTS

This thesis is based on the following article

Hara S, Kaneyama T, Inamata Y, Onodera R, and Shirasaki R (2016). Interstitial Branch Formation within the Red Nucleus by Deep Cerebellar Nuclei-Derived Commissural Axons during Target Recognition. ***The Journal of Comparative Neurology*** 524, 999-1014.

Author contributions in the above paper

All authors had full access to all the data in the study and take responsibility for the integrity of the data and the accuracy of the data analysis. Satoshi Hara, Takeshi Kaneyama and Ryota Onodera carried out the experiments. Yasuyuki Inamata. generated expression constructs. Satoshi Hara, Takeshi Kaneyama and Ryuichi Shirasaki analyzed the data, and interpreted results. Satoshi Hara and Ryuichi Shirasaki wrote the paper. Ryuichi Shirasaki conceived and supervised the project.

GENERAL INTRODUCTION

The correct wiring of neural circuits is indispensable for the central nervous system (CNS) to work properly. In the developing CNS, individual neurons extend axons toward their specific targets. The axons that have reached their target cells or their vicinity start to communicate with them and form synaptic connection to transmit the signal. This process generally begins with the generation of various types (classes) of neurons with unique characters. These neurons are initially generated from specific class of progenitor cells, the fate of which is determined, in most cases, by graded signaling of the morphogens secreted from the organizing centers (Jessell, 2000). Individual neurons then establish their unique identities by combinational expression of specific transcription factors (Shirsaki and Pfaff, 2002; Polleux et al., 2007). These intrinsic factors initiate a cascade of transcriptional interactions that ultimately leads to the expression of guidance receptors in the tip of growing axons that allow them to recognize specific guidance cues to reach their specific synaptic targets. Molecular and cellular studies to date have suggested that four types of mechanisms contribute to the guidance of growing axons toward their synaptic targets: long-range attraction (chemoattraction), long-range repulsion (chemorepulsion), short-range attraction (contact attraction), and short-range repulsion (contact repulsion) (Tessier-Lavigne and Goodman, 1996). In this scheme, the intermediate or final targets of axons secrete long-range diffusible chemoattractants that entice axons from the distance. In contrast, axons are deflected from the tissues or cells that axons normally grow away from or

avoid via a long-range action of chemorepellents secreted from them. Axons are also guided by non-diffusible cues that tightly associate with the cell surface in the environments. These cues act in principle via a contact-mediated ligand-receptor signaling to regulate the progression of axons in the local environments (Tessier-Lavigne and Goodman, 1996; Dickson, 2002). Generally, the growth cones integrate signals of multiple attractants and repellents presented in the environments that axons grow, which eventually results in the choice of specific axonal trajectories or in the recognition of specific synaptic targets.

Currently, one of the best-understood models for axon guidance is the commissural neurons in the developing spinal cord (Tessier-Lavigne and Goodman, 1996; Dickson and Zou, 2010). Commissural neurons comprise several populations depending on the location of birth along the dorsoventral axis of the spinal cord (Helms and Johnson, 2003). Among them, development of dI1-class commissural neurons, which are generated selectively from dorsal progenitors expressing the basic helix-loop-helix (bHLH) transcription factor Atoh1 (Helms et al., 1998; Helms et al., 2000), has been most extensively studied to date. In the first step of their differentiation, just after the dI1-class commissural neurons become post-mitotic, the axons of these neurons start to extend ventrally away from the roof plate via the action of chemorepellents, such as BMPs, secreted from roof plate cells at the dorsal midline of the neural tube (Augsburger et al., 1999). During their ventral elongation, these axons are then guided toward the ventral midline by Netrin1-mediated attraction via its

receptor DCC (Tessier-Lavigne et al., 1988; Kennedy et al., 1994; Serafini et al., 1994; Keino-Masu et al., 1996; Serafini et al., 1996; Dominici et al., 2017; Varadarajan et al., 2017). After commissural axons reach the ventral midline and then cross the floor plate, they dramatically change responsiveness to variety of guidance cues (Shirasaki et al., 1998; Zou et al., 2000; Nawabi and Castellani, 2011; Yam et al., 2012). Whereas commissural axons lose responsiveness to the attractant Netrin1 upon midline crossing (Shirasaki et al., 1998), they also acquire the sensitivity to the repellent Slits expressed by floor plate cells (Zou et al., 2000), those of which are considered to prevent the post-crossing axons from re-crossing the midline or from stalling at the floor plate. It should be noted that, although the repellent activity of Slit in vertebrates is regulated by its receptor Robo1 (Brose et al., 1999), the Robo1 activity itself is also under the control of another Robo family protein Robo3 in mammals that are composed of two isoforms, i.e., Robo3.1 and Robo3.2 (Sabatier et al., 2004; Chen et al., 2008; Zelina et al., 2014). In particular, Robo3.1 is expressed on the pre-crossing segment of commissural axons and inhibits the activity of Slit receptor Robo1. Owing to the silencing effect on the Slit repellent activity, commissural axons are allowed to approach and cross the floor plate. On the other hand, Robo3.2 is expressed selectively on the post-crossing segment of these axons in the same way as Robo1, thus contributing to Slit-mediated repulsion together synergistically with Robo1 (Chen et al., 2008). Then, the post-crossing commissural axons turn to extend rostrally along the longitudinal axis through the combined signaling of Wnt4 (Lyuksyutova et al., 2003) and Shh (Yam et al., 2012). Taken together, the spatial and temporal regulation of the guidance molecules and their

receptors is essential to the precise navigation of spinal commissural axons before and after crossing the floor plate.

In general, when growing axons reach the vicinity of synaptic target cells, they begin to form branches to communicate with multiple target cells. Interestingly, axonal branches show diversity in shape, size, developmental time course and so on (Gibson and Ma, 2011; Kalil and Dent, 2014). For example, in the retinotectal system, retinal ganglion cells (RGCs) extend their axons toward the tectum. These axons initially overshoot their correct terminal zone. Later, they form interstitial branches at their appropriate targets, and then the distal axons are subsequently retracted (McLaughlin et al., 2003). Axons of dorsal root ganglion (DRG) sensory neurons in the spinal cord are also found to exhibit characteristic behavior. DRG sensory neurons initially extend two axons. One axon extends peripherally to innervate muscle and skin, but the other axons extend to enter the spinal cord through the dorsal root entry zone (Wang et al., 1999). After they enter the spinal cord, each types of DRG sensory neurons project to their specific targets. For example, NGF-dependent Skin thermoreceptive/nociceptive neurons do not invade the ventral spinal cord because of repulsive signals such as Semaphorin 3A and make connections with the dorsal horn cells (Messersmith et al., 1995; Krylova et al., 2002). On the other hand, NT-3-dependent DRG neurons extend their axons toward motor neurons in the ventral spinal cord. At the limb level, Wnt3 expressed in motor neurons of the lateral motor column (LMC) specifically promotes elongation of NT-3-dependent neuron axons and

regulate the formation of terminal arborization around the motor neurons (Krylova et al., 2002). These results suggest that LMC neuron-derived Wnt3 is implicated in the target selection and recognition by the specific DRG neurons. Development of corticopontine neuron axons that project sub-cortically has also been well documented. These axons initially bypass the basilar pons and continue to grow toward the spinal cord. But, several days later, they start to initiate a delayed interstitial branching from axonal shaft around the pons (O'leary and Terashima, 1988). In vitro studies of the cortical explants using collagen matrix revealed that the explants of the basilar pons elicit the initiation and the directional growth of the interstitial branches from the cortical explants (Heffner et al., 1990; Sato et al., 1994). The extent of the branch-inducing activity was shown to be dependent on the distance between the cortical axons and the explants of the basilar pons (Sato et al., 1994). These results suggest that the interstitial branching of cortical axons toward the basilar pons is regulated by pons-derived diffusible molecules in a concentration-dependent manner. However, the nature of the pons-derived factor for cortical axon branching remains uncharacterized. On top of all that, although the mechanisms of commissural axon guidance toward, across, and around the floor plate have been particularly well documented as noted above, the process of target recognition by these axons after midline crossing remains to be addressed. Therefore, the mechanisms underlying this critical event of commissural axons on the contralateral side is currently unknown.

In this thesis, in order to gain insights into the mechanisms of the target

recognition by commissural axons on the contralateral side, here I focused on the development of commissural neurons derived from two of the deep cerebellar nuclei (DCN), the interposed and lateral nuclei in the mouse cerebellum. These commissural neurons mainly consist of excitatory glutamatergic population that is generated from Atoh1+ progenitors in the cerebellar primordium (Wang et al., 2005), and their axons share the molecular mechanisms with spinal commissural axons, particularly in the context of ventrally directed growth and midline crossing at the floor plate (Shirasaki et al., 1995; Shirasaki et al., 1996; Shirasaki et al., 1998). In addition, one of the synaptic targets of DCN neurons has already been identified as the Red Nucleus (RN) in the brainstem by electrophysiological and anatomical studies (Tsukahara et al., 1967; Chan-Palay, 1977). Especially, the DCN axon projection to the RN is shown to be topographically organized; the interposed nuclei project mainly to caudal magnocellular part in the RN and the lateral nuclei to the rostral parvocellular part (Paxinos, 2004). The connection of DCN with the RN and more rostrally with the thalamus ultimately participates in motor processing in general through involving the motor cortex and even motor neurons in the spinal cord via rubrospinal projections.

Recent study further revealed that RN cells uniquely express the POU transcription factor Brn3a during the developmental stages when DCN axons navigate around the RN (Mcevilly et al., 1996). Thus, I used the Brn3a expression as a molecular marker for the precise identification of the RN. To analyze the behavior of individual commissural axons in detail, I developed in utero electroporation system for mouse

embryos to label these axons specifically and sparsely by introducing the fluorescent protein expression vector. Here, I used the *Atoh1* enhancer-driven expression vector to specifically label DCN axons. Besides, for sparse labeling, I employed Cre/LoxP recombination-based tracing system to control the density (or the number) of fluorescently labeled cells (Badea et al., 2003; Jefferies and Livet, 2012). In order to combine the advantages of these genetic tools, I co-electroporated the *Atoh1* enhancer:: Cre vector and pCAGGS-LoxP-Stop-LoxP-GFP vector into the neural tube of the embryonic mouse hindbrain. Co-introduction of these vectors successfully induced the selective and sparse labeling of DCN axons around the RN in vivo. Thus, this genetic and sparse labeling method enabled me to examine and analyze the process of target recognition by DCN axons in detail.

Here, it was shown that post-crossing DCN axons enter the RN from the outset, and after a delay, these axons begin to form interstitial branches from the compartment of the axonal shaft selectively within the RN. This suggests that short-range locally acting cues expressed specifically within the RN may be involved in this process. Because the RN recognition by DCN axons occurs on the contralateral side during normal development, I further investigated whether midline crossing is a prerequisite for the induction of these interstitial branches within the RN by using a *Robo3* knockdown strategy in vivo. The results suggested that DCN axons have a cell-intrinsic mechanism for the generation of interstitial branches selectively within the RN irrespective of midline crossing.

REFERENCES FOR GENERAL INTRODUCTION

Augsburger A, Schuchardt A, Hoskins S, Dodd J, Butler S. 1999. BMPs as mediators of roof plate repulsion of commissural neurons. Neuron 24:127-141.

Badea TC, Wang Y, Nathans J. 2003. A noninvasive genetic/pharmacologic strategy for visualizing cell morphology and clonal relationships in the mouse. J Neurosci 23:2314–2322.

Brose K, Bland KS, Wang KH, Arnott D, Henzel W, Goodman CS, Tessier-Lavigne M, Kidd T. 1999. Slit proteins bind Robo receptors and have an evolutionarily conserved role in repulsive axon guidance. Cell 96:795-806.

Chan-Palay V. 1977. Cerebellar Dentate Nucleus: Organization, Cytology and Transmitters. (New York: Springer-Verlag)

Chen Z, Gore BB, Long H, Ma L, Tessier-Lavigne M. 2008. Alternative splicing of the Robo3 axon guidance receptor governs the midline switch from attraction to repulsion. Neuron 58:325-332.

Dickson BJ. 2002. Molecular mechanisms of axon guidance. Science 298:1959-64.

Dickson BJ, Zou Y. 2010. Navigating intermediate targets: the nervous system midline. Cold Spring Harb Perspect Biol 2:a002055.

Dominici C, Moreno-Bravo JA, Puiggros SR, Rappeneau Q, Rama N, Vieugue P, Bernet A, Mehlen P, Chédotal A. 2017. Floor plate-derived netrin1 is dispensable for commissural axon guidance. Nature 545:350-354.

Gibson DA, Ma L 2011. Developmental regulation of axon branching in the vertebrate nervous system. Development 138:183-95.

Helms AW, Abney AL, Ben-Arie N, Zoghbi HY, Johnson JE. 2000. Autoregulation and multiple enhancers control Math1 expression in the developing nervous system. Development 127:1185-1196.

Helms AW, Johnson JE. 1998. Progenitors of dorsal commissural interneurons are defined by MATH1 expression. Development 125:919-928.

Heffner CD, Lumsden AG, O'Leary DD. 1990. Target control of collateral extension and directional axon growth in the mammalian brain. Science 247:217–220.

Helms AW, Johnson JE. 2003. Specification of dorsal spinal cord interneurons. Curr Opin Neurobiol 13:42-49.

Jefferis GS, Livet J. 2012. Sparse and combinatorial neuron labeling. Curr Opin Neurobiol 22:101–110.

Jessell TM. 2000. Neuronal specification in the spinal cord: inductive signals and transcriptional codes. Nat Rev Genet 1:20-29.

Kalil K, Dent EW. 2014. Branch management: mechanisms of axon branching in the developing vertebrate CNS. Nat Rev Neurosci 15:7-18.

Kennedy TE, Serafini T, de la Torre JR, Tessier-Lavigne M. 1994. Netrins are diffusible chemotropic factors for commissural axons in the embryonic spinal cord. Cell 78:425-435.

Krylova O, Herreros J, Cleverley KE, Ehler E, Henriquez JP, Hughes SM, Salinas PC. 2002. WNT-3, expressed by motoneurons, regulates terminal arborization of neurotrophin-3-responsive spinal sensory neurons. Neuron 35:1043-1056.

Lyuksyutova AI, Lu CC, Milanesio N, King LA, Guo N, Wang Y, Nathans J, Tessier-Lavigne M, Zou Y. 2003. Anterior-posterior guidance of commissural axons by Wnt-frizzled signaling. Science 302:1984-1988.

Ma L, Tessier-Lavigne M. 2007. Dual branch-promoting and branch-repelling actions of Slit/Robo signaling on peripheral andcentral branches of developing sensory axons. J Neurosci 27:6843-6851.

Machold R, Fishell G. 2005. Math1 is expressed in temporally discrete pools of cerebellar rhombic-lip neural progenitors. Neuron 48:17–24.

McEvilly RJ, Erkman L, Luo L, Sawchenko PE, Ryan AF, Rosenfeld MG. 1996. Requirement for Brn-3.0 in differentiation and survival of sensory and motor neurons. Nature 384:574–577.

McLaughlin T, Hindges R, O'Leary DD. 2003. Regulation of axial patterning of the retina and its topographic mapping in the brain. Curr Opin Neurobiol 13:57-69.

Messersmith EK, Leonardo ED, Shatz CJ, Tessier-Lavigne M, Goodman CS, Kolodkin AL. 1995. Semaphorin III can function as a selective chemorepellent to pattern sensory projections in the spinal cord. Neuron 14:949-959.

Nawabi H, Castellani V. 2011. Axonal commissures in the central nervous system: how to cross the midline? Cell Mol Life Sci 68:2539-2553.

O'Leary DD, Terashima T. 1988. Cortical axons branch to multiple subcortical targets by interstitial axon budding: implications for target recognition and "waiting periods". Neuron 1:901-910.

Paxinos G. 2004. The Rat Nervous System. (3rd ed) (New York: Elsevier Academic

Press).

Polleux F, Ince-Dunn G, Ghosh A. 2007. Transcriptional regulation of vertebrate axon guidance and synapse formation. Nat Rev Neurosci 8:331-340.

Sabatier C, Plump AS, Le M, Brose K, Tamada A, Murakami F, Lee EY, Tessier-Lavigne M. 2004. The divergent Robo family protein rig-1/Robo3 is a negative regulator of slit responsiveness required for midline crossing by commissural axons. Cell 117:157-169.

Sato M, Lopez-Mascaraque L, Heffner CD, O'Leary DD. 1994. Action of a diffusible target-derived chemoattractant on cortical axon branch induction and directed growth. Neuron 13:791-803.

Serafini T, Kennedy TE, Galko MJ, Mirzayan C, Jessell TM, Tessier-Lavigne M. 1994. The netrins define a family of axon outgrowth-promoting proteins homologous to C. elegans UNC-6. Cell 78:409–424.

Serafini T, Colamarino SA, Leonardo ED, Wang H, Beddington R, Skarnes WC, Tessier-Lavigne M. 1996. Netrin-1 is required for commissural axon guidance in the developing vertebrate nervous system. Cell 87:1001-1014.

Shirasaki R, Katsumata R, Murakami F. 1998. Change in chemoattractant responsiveness of developing axons at an intermediate target. Science 279:105-107.

Shirasaki R, Mirzayan C, Tessier-Lavigne M, Murakami F. 1996. Guidance of circumferentially growing axons by netrin-dependent and -independent floor plate chemotropism in the vertebrate brain. Neuron 17:1079-1088.

Shirasaki R, Pfaff SL. 2002. Transcriptional codes and the control of neuronal identity. Annu Rev Neurosci 25:251-281.

Shirasaki R, Tamada A, Katsumata R, Murakami F. 1995. Guidance of cerebellofugal axons in the rat embryo: directed growth toward the floor plate and subsequent elongation along the longitudinal axis. Neuron 14:961-972.

Tessier-Lavigne M, Goodman CS. 1996. The molecular biology of axon guidance. Science.274:1123-1133.

Tessier-Lavigne M, Placzek M, Lumsden AG, Dodd J, Jessell TM. 1988. Chemotropic guidance of developing axons in the mammalian central nervous system. Nature 336:775-778.

Tsukahara N, Toyama K, Kosaka K. 1967. Electrical activity of red nucleus neurones investigated with intracellular microelectrodes. Exp Brain Res 4:18-33.

Varadarajan SG, Kong JH, Phan KD, Kao TJ, Panaitof SC, Cardin J, Eltzschig H, Kania A, Novitch BG, Butler SJ. 2017. Netrin1 produced by neural progenitors, not floor plate cells, is required for axon guidance in the spinal cord. Neuron 94:790-799.

Wang KH, Brose K, Arnott D, Kidd T, Goodman CS, Henzel W, Tessier-Lavigne M. 1999. Biochemical purification of a mammalian slit protein as a positive regulator of sensory axon elongation and branching. Cell 96:771-784.

Wang VY, Rose MF, Zoghbi HY. 2005. Math1 expression redefines the rhombic lip derivatives and reveals novel lineages within the brainstem and cerebellum. Neuron 48:31–43.

Yam PT, Kent CB, Morin S, Farmer WT, Alchini R, Lepelletier L, Colman DR, Tessier-Lavigne M, Fournier AE, Charron F. 2012. 14-3-3 proteins regulate a cell-intrinsic switch from sonic hedgehog-mediated commissural axon attraction to repulsion after midline crossing. Neuron 76:735-749.

Zelina P, Blockus H, Zagar Y, Péres A, Friocourt F, Wu Z, Rama N, Fouquet C, Hohenester E, Tessier-Lavigne M, Schweitzer J, Roest Crollius H, Chédotal A. 2014. Signaling switch of the axon guidance receptor Robo3 during vertebrate evolution. Neuron 84:1258-1272.

Zou Y, Stoeckli E, Chen H, Tessier-Lavigne M. 2000. Squeezing axons out of the gray matter: a role for slit and semaphorin proteins from midline and ventral spinal cord. Cell 102:363-375.

SUMMARY

Target recognition by developing axons is one of the fundamental steps for establishing the proper pattern of neuronal connectivity during development. However, knowledge of the mechanisms that underlie this critical event is still limited. In this study, to examine how commissural axons in vertebrates recognize their targets after crossing the midline, we analyzed in detail the behavior of post-crossing commissural axons derived from the deep cerebellar nuclei (DCN) in the developing mouse cerebellum. For this, we employed a cell-type-specific genetic-labeling approach to selectively visualize DCN axons during the time when these axons project to the red nucleus (RN), one of the well-characterized targets of DCN axons. We found that, when DCN axons initially entered the RN at its caudal end, these axons continued to grow rostrally through the RN without showing noticeable morphological signs of axon branching. Intriguingly, after a delay, DCN axons started forming interstitial branches from the portion of the axon shaft selectively within the RN. Because commissural axons acquire responsiveness to several guidance cues when they cross the midline, we further addressed whether midline crossing is a prerequisite for subsequent targeting using *Robo3* knockdown strategy. We found that DCN axons were still capable of forming interstitial branches within the RN even in the absence of midline crossing. These results therefore suggest that the mechanism of RN recognition by DCN axons involves a delayed interstitial branching, and that these axons possess an intrinsic ability to respond to the target-derived cues irrespective of midline crossing.

INTRODUCTION

The correct wiring of the nervous system depends upon a series of guidance events during neural development that gradually establish the proper pattern of neuronal connectivity. Over the past several decades, studies of neural circuit development have extensively focused on the cellular and molecular mechanisms of axon pathfinding (Dickson, 2002; Kolodkin and Tessier-Lavigne, 2011). Commissural axons, for example, have been particularly well documented for investigating the mechanisms and logic of axon guidance (Dickson and Zou, 2010; Nawabi and Castellani, 2011; Chédotal, 2014). In vertebrates, these axons initially grow toward the ventral midline in response to attractants secreted from the floor plate. Upon crossing the midline, these axons change responsiveness to guidance cues; these axons lose responsiveness to the attractants and instead become sensitive to the repellents present at the midline (Shirasaki et al., 1998; Zou et al., 2000). After exiting the floor plate, post-crossing axons turn to grow longitudinally by sensing longitudinal gradients of Wnt4 and Sonic hedgehog (Shh) (Lyuksyutova et al., 2003; Bourikas et al., 2005; Yam et al., 2012). However, the process of target recognition by these axons on the contralateral side has received less attention, and therefore the mechanisms that underlie this critical event remain poorly characterized.

In the present study, to examine how commissural axons in vertebrates recognize their targets after crossing the midline, we analyzed in detail the behavior of post-crossing commissural axons originating from the cerebellar primordium (or the cerebellar plate) during the time when these axons target the red nucleus (RN) in the

ventral midbrain, one of the major targets of these axons. We focused on this system, since not only the axonal projection pattern from the cerebellum but also their synaptic targets including the RN have been anatomically and physiologically well described, as opposed to commissural axons in the spinal cord. In particular, RN neurons uniquely express the POU transcription factor Brn3a (also known as Pou4f1) during development (McEvilly et al., 1996; Xiang et al., 1996; Nakatani et al., 2007; Prakash et al., 2009), which enables us to identify the precise location of the RN using Brn3a as a molecular marker. Besides, cerebellar commissural axons share a number of molecular mechanisms of axon guidance with spinal commissural axons when these axons grow toward and cross the floor plate (Tessier-Lavigne et al., 1988; Kennedy et al., 1994; Serafini et al., 1994; Shirasaki et al., 1995; Shirasaki et al., 1996), including an essential requirement of Robo3 for midline crossing in vivo (Sabatier et al., 2004; Tamada et al., 2008).

It should be noted that the cerebellar commissural axons that cross the floor plate are known to correspond to those derived from two of the deep cerebellar nuclei (DCN), the interposed and lateral nuclei in the cerebellum (Shirasaki et al., 1995; Altman and Bayer, 1997). It is also known that the DCN consists mainly of excitatory glutamatergic and inhibitory GABAergic populations (Batini et al., 1992). Physiological and anatomical studies have suggested that glutamatergic population projects rostrally to the red nucleus (RN) and thalamus (Tsukahara et al., 1967; Toyama et al., 1970; Chan-Palay V. 1977; Ito, 1984; Brodal, 1992; Schwarz and Schmitz, 1997; Jiang et al., 2002; Paxinos, 2004), and GABAergic population projects caudally to the inferior olive

(Fredette and Mugnaini, 1991; Bengtsson and Hesslow, 2006). Importantly, genetic fate mapping in the cerebellar primordium demonstrated that glutamatergic and GABAergic DCN neurons are generated from distinct progenitor cells that uniquely express the basic helix-loop-helix (bHLH) transcription factor Atoh1 and Ptf1a, respectively (Hoshino et al., 2005; Machold and Fishell, 2005; Wang et al., 2005). Thus, in this study, we employed the *Atoh1* enhancer element-based conditional expression system to selectively visualize individual glutamatergic DCN neurons in mice. Furthermore, we combined this genetic-labeling approach with Brn3a immunohistochemistry for the precise identification of the RN. The *Atoh1* enhancer-based genetic tool was introduced by an in vivo electroporation technique developed for mouse embryos (Tabata and Nakajima, 2001; Saito, 2006; Shimogori and Ogawa, 2008). In addition, because commissural axons acquire responsiveness to several guidance cues when they cross the midline, we also addressed whether midline crossing is a prerequisite for reception of target-derived cues normally received by post-crossing DCN axons. For this, we prevented midline crossing by DCN axons using *Robo3* knockdown strategy in vivo.

MATERIALS AND METHODS

Mice

Timed pregnant ICR mice were obtained from Japan SLC (Hamamatsu, Japan). Noon of the day on which a vaginal plug was found was designated as embryonic day 0.5 (E0.5). All experiments were performed in accordance with the guidelines of the animal welfare committees of Osaka University and the Japan Neuroscience Society.

Plasmids

For selective and sparse labeling of DCN neurons that are generated from Atoh1-positive progenitors, we used Cre/LoxP-based strategy in which the *Atoh1* enhancer element (Helms et al., 2000) was linked to Cre recombinase that conditionally labels cells when co-introduced with a plasmid containing *gfp* proceeded by a floxed stop-cassette. In recent years, an employment of enhancer elements to direct expression of reporter genes in neurons of interest is a widely used approach for tracing axonal trajectories in the nervous system (Miyoshi and Fishell, 2006). Moreover, Cre/LoxP recombination-based tracing system enables sparse labeling (i.e., low density labeling) of genetically defined cells (Badea et al., 2003; Young and Feng, 2004; Rotolo et al., 2008; Jefferis and Livet, 2012). In this study, we co-electroporated *Atoh1* enhancer-driven Cre (*Atoh1 enhancer::Cre*) vector together with pCAG-LoxP-CAT-LoxP-AcGFP1 vector into the cerebellar plate. Briefly, *Atoh1 enhancer::Cre* vector was generated from Atoh1-Venus-Neo/pBluescript SK+ plasmid (generous gift from Dr. Y. Sasai, Riken, Kobe, Japan) (Helms et al., 2000; Su et al.,

2006) by replacing an open reading frame (ORF) of *Venus* with that of *Nuclear Cre* (*NCre*) isolated from pNC/pTK174 vector (generous gift from Dr. M. Sato, Kagoshima University, Kagoshima, Japan) (Nakamura et al., 2008). To reflect the endogenous temporal activity of the *Atoh1* enhancer in the transfected cells, we fused a protein-degradation sequence (hCL1-hPEST sequence) isolated from the Rapid Response pGL4 Reporter Vector (Promega) to the C-terminus of NCre. We then replaced the SV40 early poly(A) signal with the SV40 late poly(A) signal and a synthetic poly(A) signal, both of which were isolated from the pGL4 Luciferase Reporter Vector (Promega), to increase the efficiency of transcription termination and polyadenylation of the NCre transcripts. To generate pCAG-LoxP-CAT-LoxP-AcGFP1 vector, we first amplified a fragment of *LoxP-CAT-LoxP* sequence from pCT vector (generous gift from Dr. M. Sato, Kagoshima University) (Sato et al., 2000; Nakamura et al., 2008) and added multiple cloning site (MCS) downstream of the second LoxP site of this fragment. The *LoxP-CAT-LoxP-MCS* fragment was then inserted into the *Xba*I and *Eco*RI sites of pCAGGS vector (generous gift from Dr. J. Miyazaki, Osaka University, Osaka, Japan) (Niwa et al., 1991). Next, a fragment containing three tandem repeats of SV40 late poly(A) signal and a synthetic poly(A) signal that were isolated similarly from the pGL4 Reporter Vector (Promega) was placed downstream of the *CAT* gene. Then, an ORF of *AcGFP1* from pIRES2-AcGFP1 vector (Clontech) was inserted into the *Kpn*I site of the MCS. *Atoh1* enhancer-driven ZsGreen1 (*Atoh1 enhancer::ZsGreen*) vector was generated similarly from the Atoh1-Venus-Neo/pBluescript SK+ plasmid by replacing an ORF of *Venus* with that of

ZsGreen1 (Clontech). All junctions were confirmed by sequencing.

In vivo electroporation

To visualize the trajectory of DCN axons in mice, in vivo electroporation was carried out as described (Saba et al., 2003; Inamata and Shirasaki, 2014). In brief, after plasmid vectors were injected into the fourth ventricle of mouse embryos, electric pulses were applied to the cerebellar plate (CP) using square pulse electroporator (CUY-21, Bex) with a pair of 3 mm diameter platinum electrode (CUY650P3, NEPA GENE) (Fig. 1A). The introduction of the expression plasmids using in vivo electroporation was performed at E11.5 since the majority of DCN neurons are generated at around this stage (Pierce, 1975; Altman and Bayer, 1978; Machold and Fishell, 2005). *Robo3* knockdown was carried out using in vivo electroporation of *Robo3*-specific siRNA as described (Inamata and Shirasaki, 2014). The siRNA and the Cre/LoxP vectors described above were co-electroporated. Several days after the electroporation, the electroporated embryos were taken out from the mother, flat-mounted and fixed with 4% paraformaldehyde (PFA) in 0.1M phosphate buffer (pH7.4) for 2 hours at 4ºC and subjected to immunohistochemistry for further analyses (Fig. 1B-C). The procedure for flat-mounted midbrain/hindbrain preparations was described previously (Shirasaki et al., 1995), except that, in embryos older than E15.5, one side of the dorsal midbrain and the diencephalon was removed to observe the entire trajectory of DCN axons growing toward the thalamus. The flat-mounted preparations enable ready recognition of the entire trajectories of labeled axons in 2D plane, together with their relation to the

location of the RN as well as to the circumferential and longitudinal axes of the developing brain (Shirasaki et al., 1995).

Immunohistochemistry

Whole-mount immunohistochemistry on flat-mounted midbrain/hindbrain preparations was performed as described (Shirasaki et al., 2006; Inamata and Shirasaki, 2014). The Vector MOM Immunodetection Kit (Vector Laboratories) was used when primary antibodies from mouse were used. The AcGFP and ZsGreen signals were enhanced using anti-GFP and anti-ZsGreen antibodies, respectively. The region of the RN was defined by the expression of Brn3a in the ventral midbrain as previously reported (McEvilly et al., 1996; Xiang et al., 1996; Prakash et al., 2009). Images were taken by a fluorescence microscopy (Olympus, BX61N) with a high-resolution digital cooled charged-coupled device (CCD) camera (Hamamatsu Photonics, ORCA-AG) and by a confocal laser scanning microscopy (LSM) (Olympus, Fluoview FV300).

Antibody Characterization

The primary antibodies used in this study, their sources, and their working dilutions are summarized in Table 1. The mouse monoclonal (IgG1) to Brn3a (RRID:AB_94166) was obtained from Millipore and raised against amino acids 186-224 of Brn3a fused to the T7 gene 10 protein. The Bran3a antibody shows no reactivity to Brn3b or Brn3c by Western blot and no reactivity to Brn3a knockout mice (manufacture's technical information). Its specificity for mouse red nucleus neurons in the ventral midbrain has

Table 1

Antigen	**Description of Immunogen**	**Source, Host Species, Cat. #, Clone or Lot#, RRID**	**Concentration Used**
Brn3a	Synthetic peptide corresponding to amino acids 186-224 of human Brn3a	Millipore, mouse monoclonal, Cat# MAB1585, RRID:AB_94166	1:600
Lhx9	Synthetic peptide mapping within an internal region of human Lhx9	Santa Cruz Biotechnology, goat polyclonal, Cat# sc-19350, RRID:AB_2249920	1:200
GFP	GFP isolated from *Aequorea victoria*	Life Technologies, rabbit polyclonal, Cat# A11122, RRID:AB_221569	1:2000
ZsGreen	Recombinant full-length ZsGreen protein	Clontech, rabbit polyclonal, Cat# 632474, RRID:AB_2491179	1:500

previously been documented (Nakatani et al., 2007; Ono et al., 2010; Inamata and Shirasaki, 2014).

The goat polyclonal anti-Lhx9 (RRID:AB_2249920) was purchased from Santa Cruz Biotechnology. It was developed by using a synthetic peptide from an internal region of human Lhx9. The antibody recognizes a single band of 44 kDa on a Western blot of HeLa-cell nuclear extract (manufacture's technical information). This antibody has been used to specifically visualize nuclei of tectobulbar neurons in the mouse midbrain (Inamata and Shirasaki, 2014).

The rabbit polyclonal anti-GFP (RRID:AB_221569) was obtained from Life Technologies. It was raised against GFP isolated directly from *Aequorea victoria*, and was further purified by ion-exchange chromatography (manufacture's technical information). The antibody has been used previously to label GFP-expressing cells selectively in the embryonic mouse brain transfected with GFP-expression plasmids (Inamata and Shirasaki, 2014).

The rabbit polyclonal anti-ZsGreen (RRID:AB_2491179) was obtained from Clontech Laboratories. This antibody was raised against recombinant full-length ZsGreen. It recognizes a band of approximately 30-35 kDa corresponding to ZsGreen on a Western blot of lysate made from an HEK 293 cell line stably expressing ZsGreen. A band of this size is not detected in the lysate of untransfected HEK 293 cells (manufacture's technical information). The antibody has been used previously to label ZsGreen-expressing cells selectively in the embryonic mouse midbrain transfected with ZsGreen-expression plasmids (Inamata and Shirasaki, 2014).

Quantification

Flat-mounted preparations of the electroporated embryos were subjected to double-label immunohistochemistry for expression of Brn3a and GFP. *z*-stack LSM images of 5 μm-thickness optical sections were used to analyze the entire trajectory of GFP-labeled DCN axons within and around the RN in the flat-mounted preparations. *xy*-plane optical section images obtained from the *z*-stack LSM images were then used for further detailed analysis of the behavior of individual GFP-labeled DCN axons visualized by Cre/LoxP-mediated cell-type-specific sparse labeling. ImageJ software (NIH, Bethesda, MD; RRID:nif-0000-30467) (Schneider et al., 2012) was used to count the number of GFP-labeled axons possessing branches within and around the RN from a series of superimposed *xy*-plane LSM images. Similarly, using ImageJ software, the length of GFP-labeled branches was measured and the position of branching points along the axon was determined. The number of branches was counted according to the length of the branches at 10 μm intervals. GFP-labeled protrusions (5 μm or longer) from the main axon were classified as branches, and those less than 5 μm in length were excluded from the analysis since it has been shown that these short branches are unstable and rapidly retract (Cohen-Cory and Fraser, 1995).

RESULTS

Tracing DCN axons in mice by Atoh1 enhancer-driven fluorescent reporter

Using the lipophilic fluorescent tracer DiI, we have previously shown that post-crossing DCN axons make a rostral turn to grow longitudinally, reaching in proximity to the RN at around E15 in the rat embryo (Shirasaki et al., 1995; Shirasaki and Murakami, 2001). Because the DiI implantation into the cerebellar plate (CP) late in embryonic development can also potentially cause axonal labeling other than DCN axons due to its non-specific labeling, here we employed a genetic-labeling strategy to selectively visualize DCN axons at around the time when DCN axons reach the RN. For this, we first introduced *Atoh1 enhancer::ZsGreen* vector into the CP using in vivo electroporation at E11.5 in mice, and analyzed the overall development of DCN axons in flat-mounted preparations at E14 (Fig. 1A-C). We found that cohort of ZsGreen-labeled DCN axons crossed the floor plate and reached the RN at this stage (Fig. 1D-F), consistent with the previous reports using DiI in rats as noted above. We then analyzed the behavior of DCN axons in relation to the precise location of the RN using confocal LSM. We found that DCN axons entered the RN at its caudal end and continued to grow rostrally within the RN (Fig. 1G-L).

To analyze in detail the behavior and the morphology of individual DCN axons, we next employed Cre/LoxP-based cell-type-specific sparse labeling in which Cre expression is under the control of the *Atoh1* enhancer. As expected, this enabled us to monitor the behavior of sparsely-labeled individual DCN axons growing within the RN (Fig. 2). In this sparsely labeled condition (compare Fig. 2G with Fig. 1G), we found that some of

Figure 1

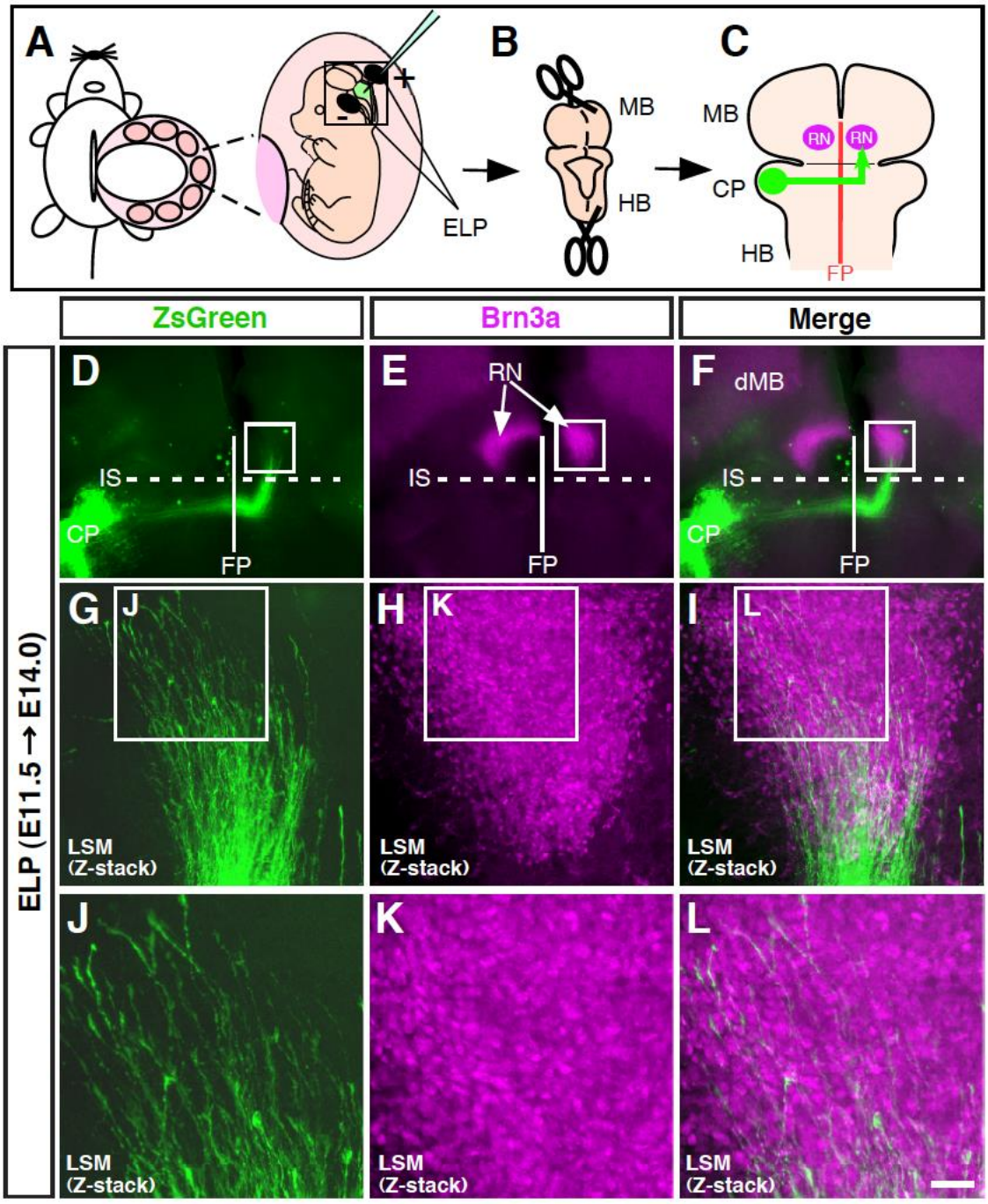
A
B
C
MB
HB
ELP
MB
CP
HB
RN
RN
FP
ZsGreen
Brn3a
Merge
ELP (E11.5 → E14.0)
D
E
F
RN
dMB
IS
CP
FP
G
J
H
K
I
L
LSM
(Z-stack)

Figure 1. Trajectory of post-crossing DCN axons revealed by mouse in vivo electroporation.

(A-C) Schematic showing an outline of experimental procedures for the analysis of DCN axon development in mice. (A) In vivo electroporation was carried out in the cerebellar plate (CP) at E11.5. (B,C) Several days after electroporation, the electroporated embryos were taken out from the mother. The neural tube including the midbrain and hindbrain was cut along the roof plate, and flat-mounted in order to analyze the entire trajectory of labeled axons. After fixation with 4% paraformaldehyde, Brn3a immunohistochemistry on the flat-mounted preparations was performed to identify the location of the red nucleus (RN). (D-F) Trajectory of DCN axons at E14 revealed by in vivo electroporation of *Atoh1 enhancer::ZsGreen* vector. The Brn3a expression in the ventral midbrain denotes the location of the RN (arrows). (G-I) Higher-magnification images of white rectangles in D-F, respectively, but showing a *z*-stack image of 22 optical sections (5 μm thickness) obtained by confocal LSM. The total thickness of the optical sections encompasses the thickness of the RN identified by Brn3a immunohistochemistry. ZsGreen-labeled DCN axons enter the RN at its caudal end at around E14. (J-L) High-power views of white rectangles in G-I, respectively. After entering the RN, DCN axons continue to grow rostrally within the RN. CP, cerebellar plate; dMB, dorsal midbrain; ELP, electroporation; FP, floor plate; HB, hindbrain; IS, isthmus; LSM, laser scanning microscopy; MB, midbrain; RN, red nucleus. Scale bar, 300 μm in (D)-(F), 50 μm in (G)-(I), 25 μm in (J)-(L).

Figure 2

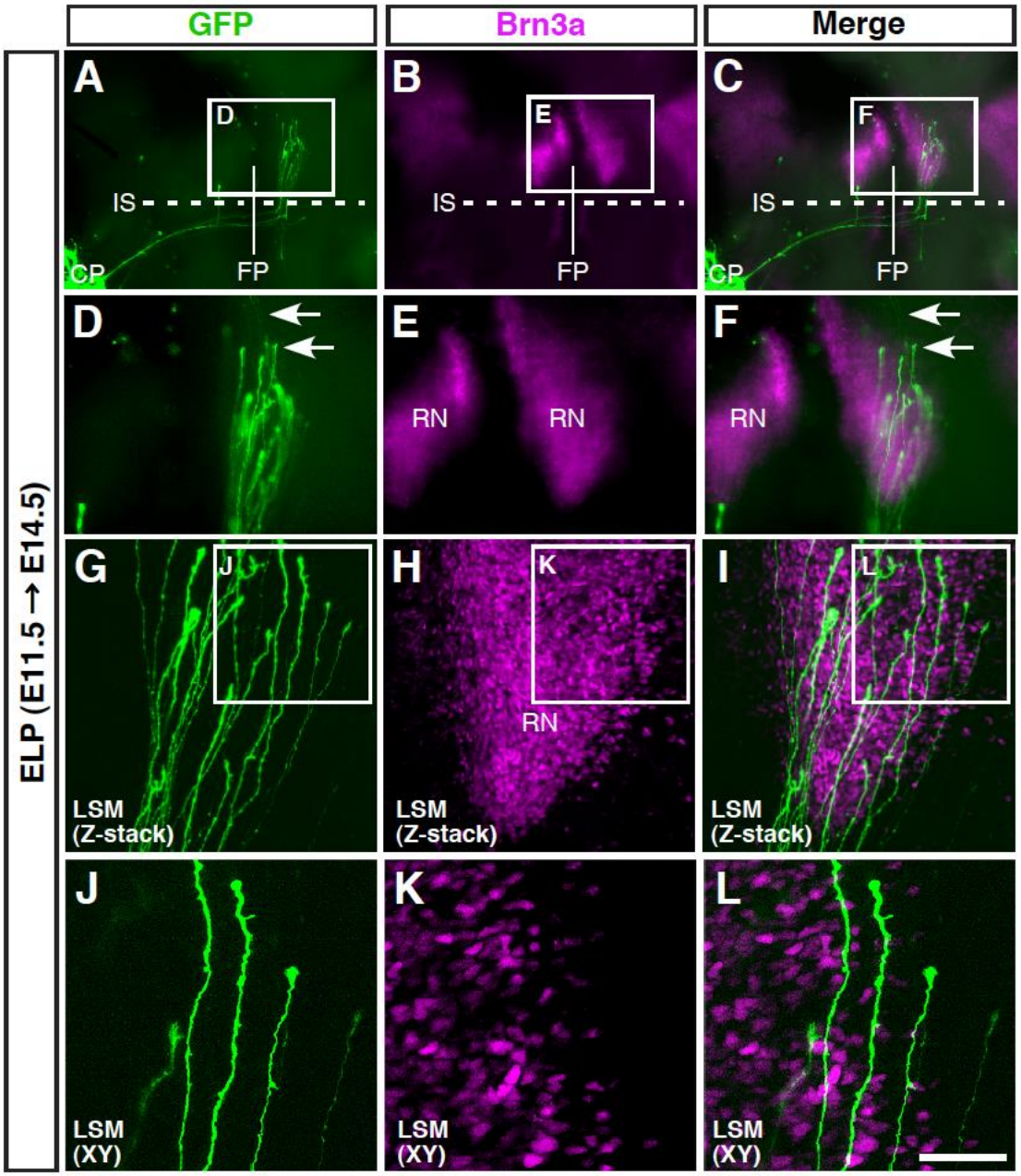
GFP
Brn3a
Merge
ELP (E11.5 → E14.5)
A
B
C
D
E
F
IS
CP
FP
RN
G
H
I
J
K
L
LSM
(Z-stack)
LSM
(XY)

Figure 2. DCN axons initially grow rostrally through the RN without branching.

(A-L) Behavior of GFP-labeled DCN axons revealed by Cre/LoxP-based cell-type-specific sparse labeling. Co-electroporation of *Atoh1 enhancer::Cre* and *pCAG-LoxP-stop-LoxP-GFP* vectors was performed at E11.5. (A-C) Entire trajectory of GFP-labeled DCN axons at E14.5. (D-F) Higher-magnification views of white rectangles in A-C, respectively. Some of the DCN axons have already extended through and overshot the RN (arrows). (G-I) *z*-stack LSM images of 32 optical sections (5 μm thickness), showing DCN axons growing rostrally within the RN at E14.5. The total thickness optically scanned by LSM corresponds to the thickness of the RN. (J-L) High-power images of white boxes in G-I, respectively, but showing an *xy*-plane of LSM image. Typical DCN axons including their axonal growth cones are shown. DCN axons growing within the RN exhibit no morphological signs of branching at this stage. CP, cerebellar plate; FP, floor plate; IS, isthmus; LSM, laser scanning microscopy; RN, red nucleus. Scale bar, 240 μm in (A)-(C), 120 μm in (D)-(F), 100 μm in (G)-(I), 50 μm in (J)-(L).

the growth cones of GFP-labeled DCN axons had already passed through the RN (Fig. 2F, arrows). Detailed analysis of the behavior of individual GFP-labeled DCN axons on the *z*-stack images (Fig. 2G-I) as well as those on the *xy*-plane (Fig. 2J-L) using confocal LSM clearly showed that, when DCN axons initially entered the RN, these axons continued to grow rostrally through the RN without showing noticeable morphological signs of axon branching. Quantification of the ratio of individual GFP-labeled axons with branches showed that few DCN axons had branches within the RN at this stage (Fig. 5A). These results suggest that the growth cone of DCN axons seemingly ignore the RN when they initially enter and grow within the RN.

Emergence of interstitial branches by DCN axons within the RN

The behavior of DCN axons described above is reminiscent of that of sensorimotor cortical axons from layer 5 neurons, whose recognition of subcortical targets occurs via a delayed interstitial branching (O'Leary and Terashima, 1988; O'Leary et al, 1990; Kalil and Dent, 2014). Corticopontine axons in rodents, for example, initially bypass the basilar pons, but after a delay, they develop interstitial branches from the axon shaft overlying the basilar pons (O'Leary and Terashima, 1988; Bastmeyer and O'Leary, 1996). This prompted us to further examine the detailed behavior of DCN axons at later stages using Cre/LoxP-based cell-type-specific sparse labeling, with special attention to the axon shaft within the RN. Intriguingly, at E15.5 (Fig. 3), we found that DCN axons started to give rise to interstitial branches along their shafts within the RN (Fig. 3I, arrowheads). At E16.5, we found that these interstitial branches continued to grow in

Figure 3

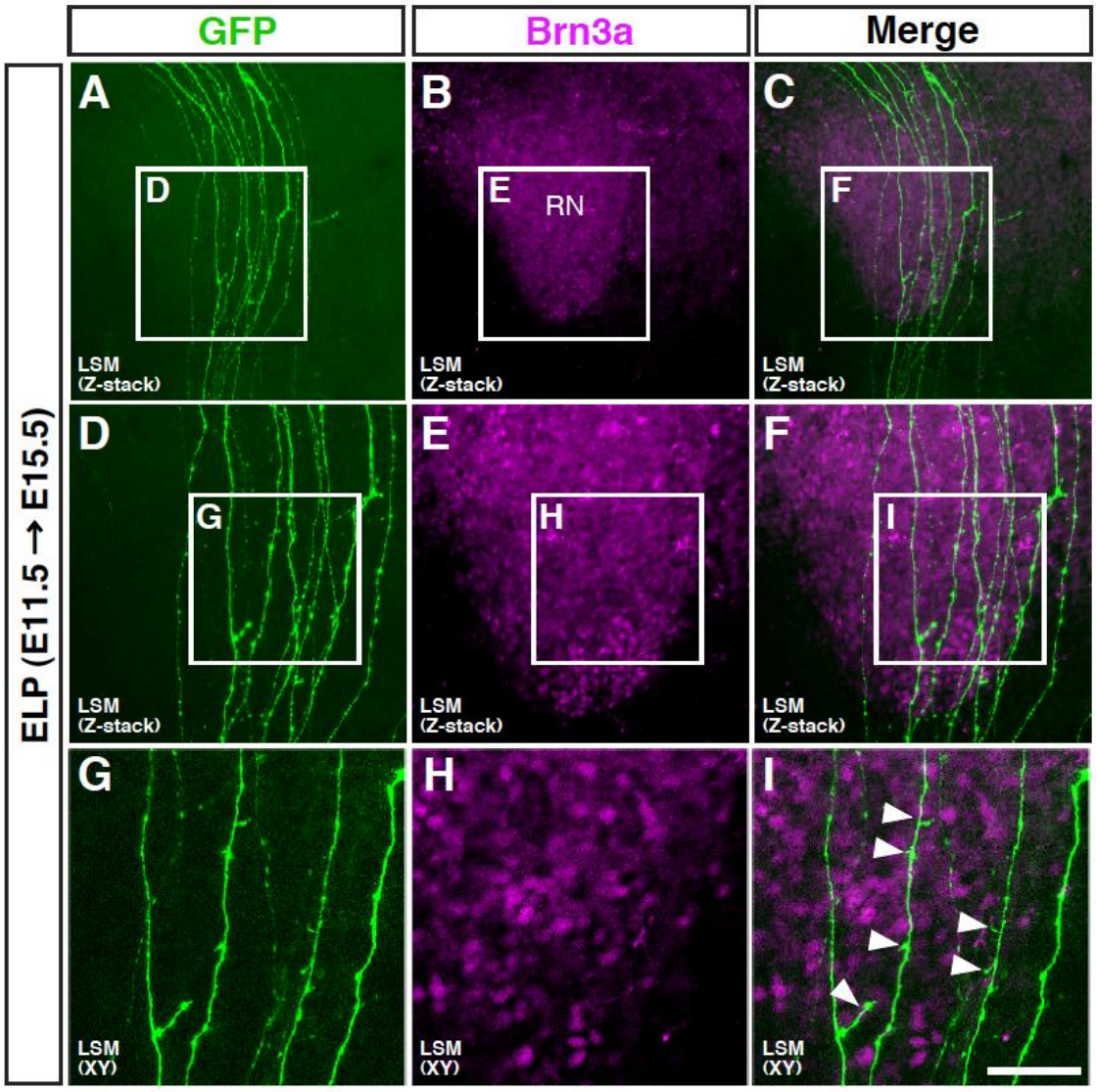
GFP
Brn3a
Merge
ELP (E11.5 → E15.5)
A
B
C
D
E
RN
F
LSM
(Z-stack)
D
E
F
G
H
I
LSM
(Z-stack)
G
H
I
LSM
(XY)

Figure 3. Delayed interstitial branching by DCN axons within the RN.

(A-I) Behavior of GFP-labeled DCN axons within the RN at E15.5. (A-C) *z*-stack LSM images of 10 optical sections (10 μm thickness), including the entire trajectory of GFP-labeled DCN axons within and around the RN. Most of the DCN axons at this stage have already overshot the RN to grow rostrally toward the thalamus. (D-F) High-power views of white rectangles in A-C, respectively, showing a *z*-stack image of 14 optical sections (5 μm thickness) captured by confocal LSM. The optical sections were taken to trace the entire trajectory of GFP-labeled DCN axons within the RN. (G-I) Higher-magnification images of white boxes in D-F, respectively, but showing an *xy*-plane of LSM image. Note that some DCN axons start forming interstitial branches from the portion of the axon shaft within the RN (arrowheads). Rostral is to the top and medial (ventral) is to the left. LSM, laser scanning microscopy; RN, red nucleus. Scale bar, 200 μm in (A)-(C), 100 μm in (D)-(F), 50 μm in (G-I).

length within the RN (Fig. 4G, white oval). Quantification analyses also indicated that the ratio of the number of DCN axons having branches within the RN as well as the length of the branches increased dramatically with age compared with those at E14.5 (Fig. 5A,B). Moreover, at E17.5, we found that, after exiting the ventral midbrain region, DCN axons extended toward their final targets in the dorsal thalamus without having interstitial branches (Fig. 4J-N). Together, these results suggest that DCN axons develop axon collaterals within the RN by a delayed interstitial branching from the axon shaft behind the leading growth cone.

We next focused our attention on the properties of axon collaterals generated within the RN. We first examined whether there is any rostrocaudal pattern and/or preference of branch formation within the RN. For this, we subdivided the RN into the rostral and caudal half, and analyzed the location of the branch points in each subdivision. However, we found no obvious differences of branch emergence along the rostrocaudal axis of the RN (Fig. 5C). We further examined whether there is any preference in the orientation of axon collaterals within the RN in relation to the mediolateral axis of the RN. For this analysis, we subdivided the RN into three parts: the medial (ventral), intermediate, and lateral (dorsal) third. Interestingly, we found that the collateral branches formed in the medial and intermediate domains of the RN significantly tended to extend laterally away from the floor plate, whereas those formed in the lateral domain did not (Fig. 5D). Considering that the ventral two-thirds of the RN is located closer to the floor plate, the orientation preference observed in those

Figure 4

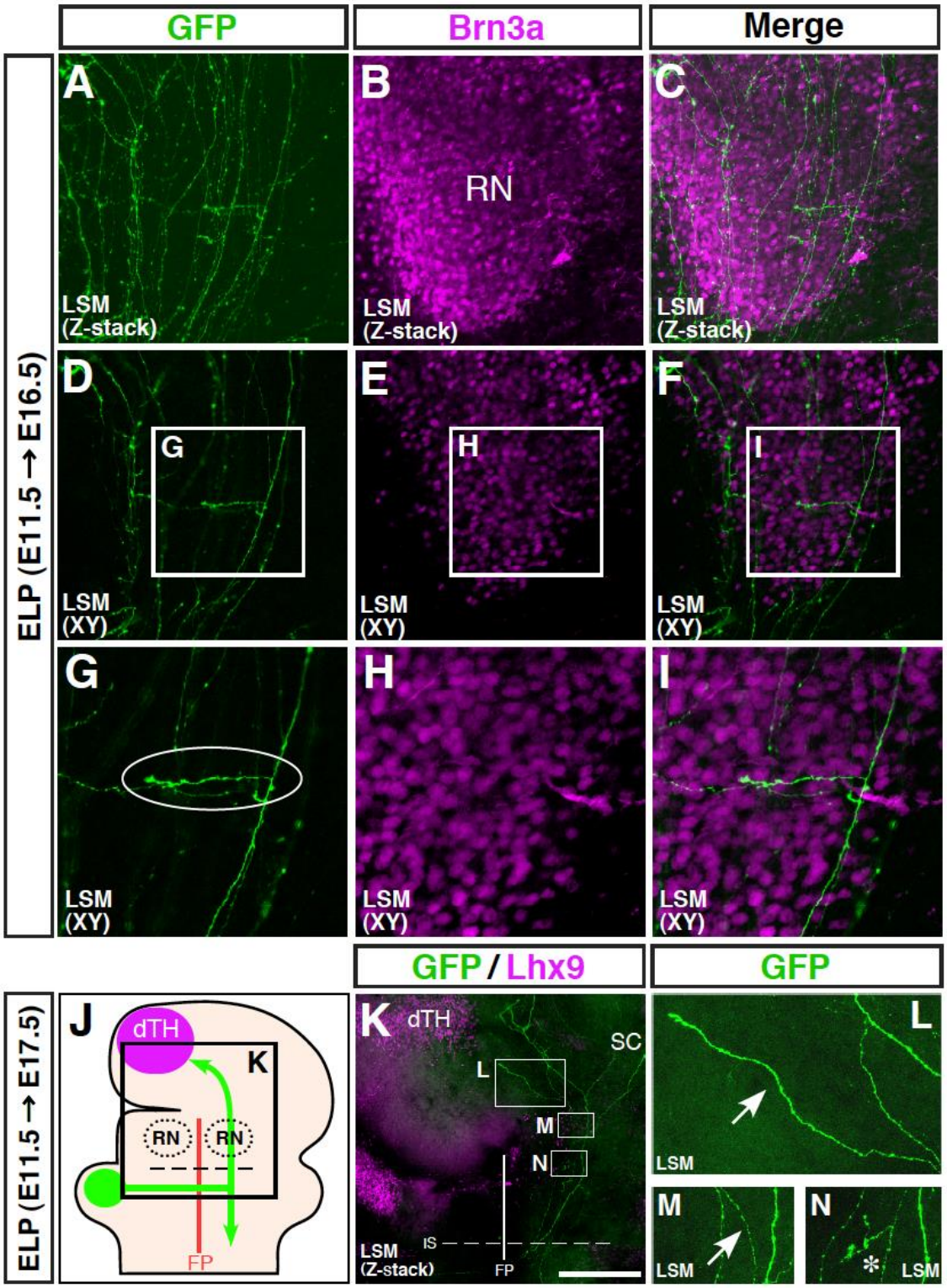
GFP
Brn3a
Merge
ELP (E11.5 → E16.5)
A
B
C
RN
LSM
(Z-stack)
D
E
F
G
H
I
LSM
(XY)
ELP (E11.5 → E17.5)
GFP / Lhx9
GFP
J
dTH
K
RN
FP
SC
L
M
N
IS
LSM
(Z-stack)

Figure 4: Elongation of interstitial branches within the RN.

(A-I) Behavior of DCN axons observed within the RN at E16.5. The *Atoh1* enhancer-based conditional GFP expression vectors were electroporated at E11.5, and detailed behavior of GFP-labeled DCN axons was analyzed in flat-mounted preparations at E16.5. (A-C) *z*-stack LSM images of 31 optical sections (5 μm thickness), including the entire trajectory of GFP-labeled DCN axons within the RN. The RN region was identified by Brn3a immunohistochemistry. (D-F) Representative images of *xy*-plane optical sections obtained from a *z*-stack LSM image shown in A-C. (G-I) Higher-magnification views of white rectangles in D-F, respectively. The white oval in G denotes an example of a long-extending interstitial branch (approx. 65 μm in length). (J-N) Behavior of DCN axons observed in the ventral midbrain and around the dorsal thalamus at E17.5. (J) Schematic showing an overall trajectory of DCN axons at E17.5. Lhx9 immunohistochemistry on the flat-mounted preparations was performed to identify the location of dorsal thalamic nuclei including the ventrolateral nucleus (Nakagawa and O'Leary, 2001). (K) Higher-magnified image of black rectangle in J, showing a *z*-stack image of 19 optical sections (10 μm thickness) obtained by confocal LSM. The entire trajectory of a single DCN axon extending from the cerebellar plate to the area around the dorsal thalamus via the RN is shown. At this stage, the DCN axon has not yet entered the dorsal thalamic nuclei. In this preparation, DCN axons projecting to the superior colliculus (Paxinos, 2004) were also labeled. (L-N) Higher-magnification views of white rectangles in K, respectively. Arrow in L and M, respectively, corresponds to the same DCN axon possessing an interstitial branch

(asterisk in N) in the ventral midbrain where the RN is located. After exiting the ventral midbrain region, the DCN axon extends toward the dorsal thalamus without forming interstitial branches. Rostral is to the top and medial (ventral) is to the left (A-I). dTH, dorsal thalamus; FP, floor plate; IS, isthmus; LSM, laser scanning microscopy; RN, red nucleus; SC, superior colliculus. Scale bar, 100 μm in (A-F, L-N), 50 μm in (G-I), 400 μm in (K).

domains may reflect responsiveness of axon collaterals to floor-plate repellents to which commissural axons become sensitive only after crossing the floor plate.

Spatially restricted generation of interstitial branches by DCN axons

Although the above results indicate that DCN axons initiate delayed interstitial branching within the RN, they do not directly address whether these branches emerge selectively within the RN from the outset. To address this issue, we first analyzed the location of interstitial branches along the axon shaft after DCN axons had already entered the RN at E16.5 (Fig. 6). For this, we categorized DCN axons into two groups: one having branches from the portion of the axon shaft before entering the RN (here referred to as "Pre") (Fig. 6B-F), and the other having branches from the segment of the axon shaft only within the RN (here referred to as "Post") (Fig. 6B,G-J). Quantification of the ratio of "Pre-" and "Post-" groups of DCN axons indicated that the majority of DCN axons possessed interstitial branches only within the RN (Fig. 6C-K, arrowheads). We next examined whether DCN axons transiently develop interstitial branches before the leading growth cone of DCN axons reach the RN. To assess this, we analyzed the shaft of DCN axons whose leading growth cones had not yet entered the RN at E14.5 (Fig. 7A,B). We found that, before the axonal growth cone of DCN axons reached the RN, these axons possessed few branches from the axon shaft (Fig. 7B-G). Together with the results described above (Fig. 4J-N), these results suggest that, from the outset, DCN axons form interstitial branches selectively within the RN.

Figure 5

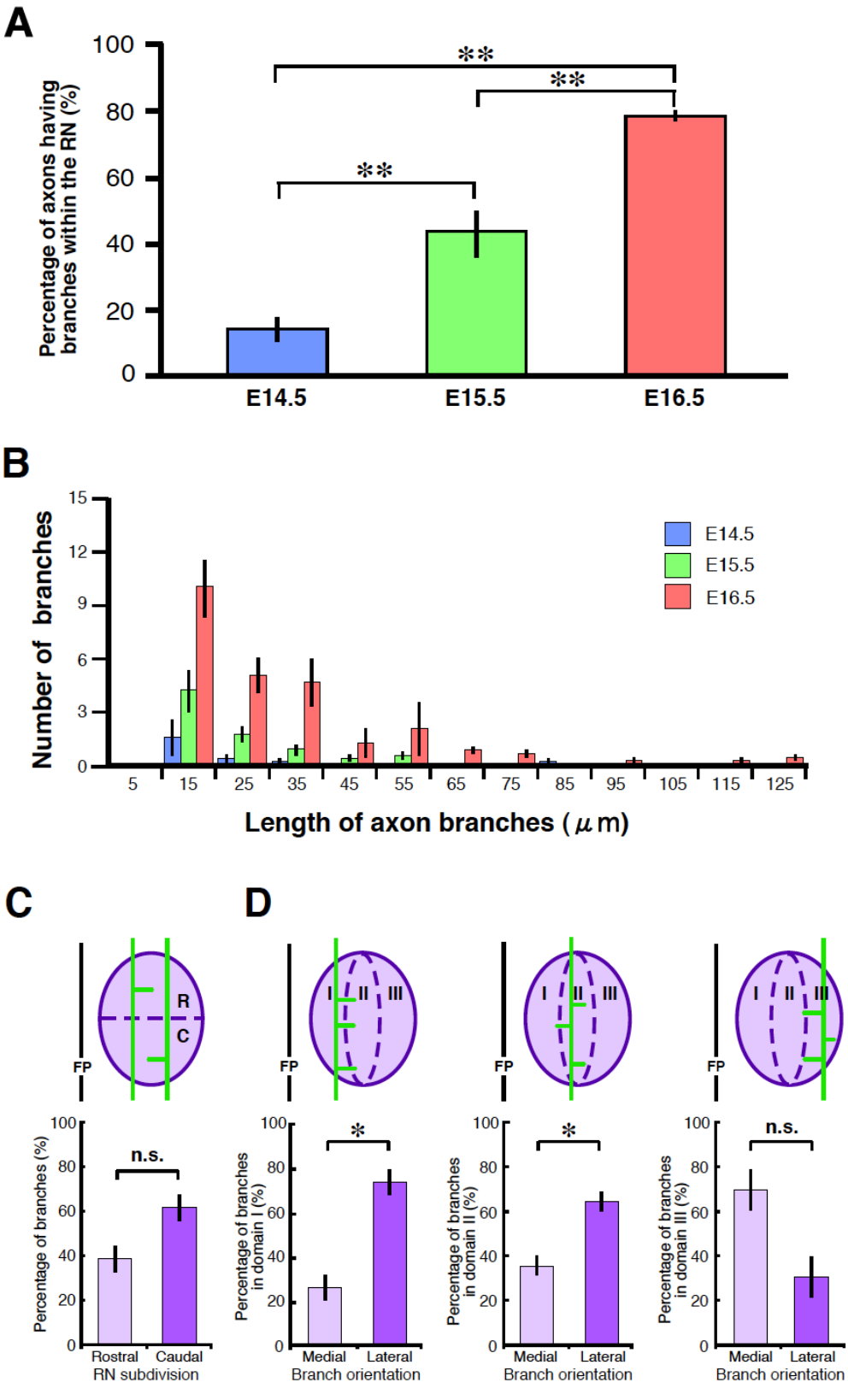
A
Percentage of axons having branches within the RN (%)
100
80
60
40
20
0
**
**
**
E14.5
E15.5
E16.5
B
Number of branches
15
12
9
6
3
0
E14.5
E15.5
E16.5
5
15
25
35
45
55
65
75
85
95
105
115
125
Length of axon branches (μm)
C
D
FP
R
C
I
II
III
Percentage of branches (%)
n.s.
Rostral
Caudal
RN subdivision
Percentage of branches in domain I (%)
*
Medial
Lateral
Branch orientation
Percentage of branches in domain II (%)
*
Medial
Lateral
Branch orientation
Percentage of branches in domain III (%)
n.s.
Medial
Lateral
Branch orientation

Figure 5. Quantification of the development of interstitial branches.

(A) Histogram showing the ratio of GFP-labeled DCN axons having branches within the RN at different developmental stages. At E14.5 when DCN axons initially enter the RN, these axons rarely give off branches. Strikingly, at E15.5 and older, the majority of DCN axons develop interstitial branches within the RN. (B) Histogram showing the number and the length of interstitial branches by DCN axons within the RN at different developmental stages. The length as well as the number of branches within the RN increases with age. (C) Quantification of the location of branch points along the rostrocaudal axis of the RN. The RN was subdivided into the rostral and caudal half, and evaluated rostrocaudal preference of branch formation within the RN at E16.5. (D) Quantification of mediolateral preference in the orientation of collateral branches within the RN. For this analysis, the RN was subdivided into three parts: the medial (domain I), intermediate (domain II), and lateral third (domain III). Then, the mediolateral preference of the branch direction within each domain of the RN was evaluated at E16.5. Note that collateral branches formed in the medial and intermediate domains of the RN have a significant preference to grow laterally away from the floor plate. Error bars indicate s.e.m. Statistical significance was determined by Student's *t*-test (*P<0.05, **P<0.01, n.s., not significant). The average number of axons analyzed per embryo was approximately 14 at E14.5 (blue, n=6 embryos), 16 at E15.5 (green, n=6 embryos), and 23 at E16.5 (red, n=5 embryos), respectively. Rostral is to the top and medial (ventral) is to the left (C, D). C, caudal; FP, floor plate; R, rostral.

Figure 6

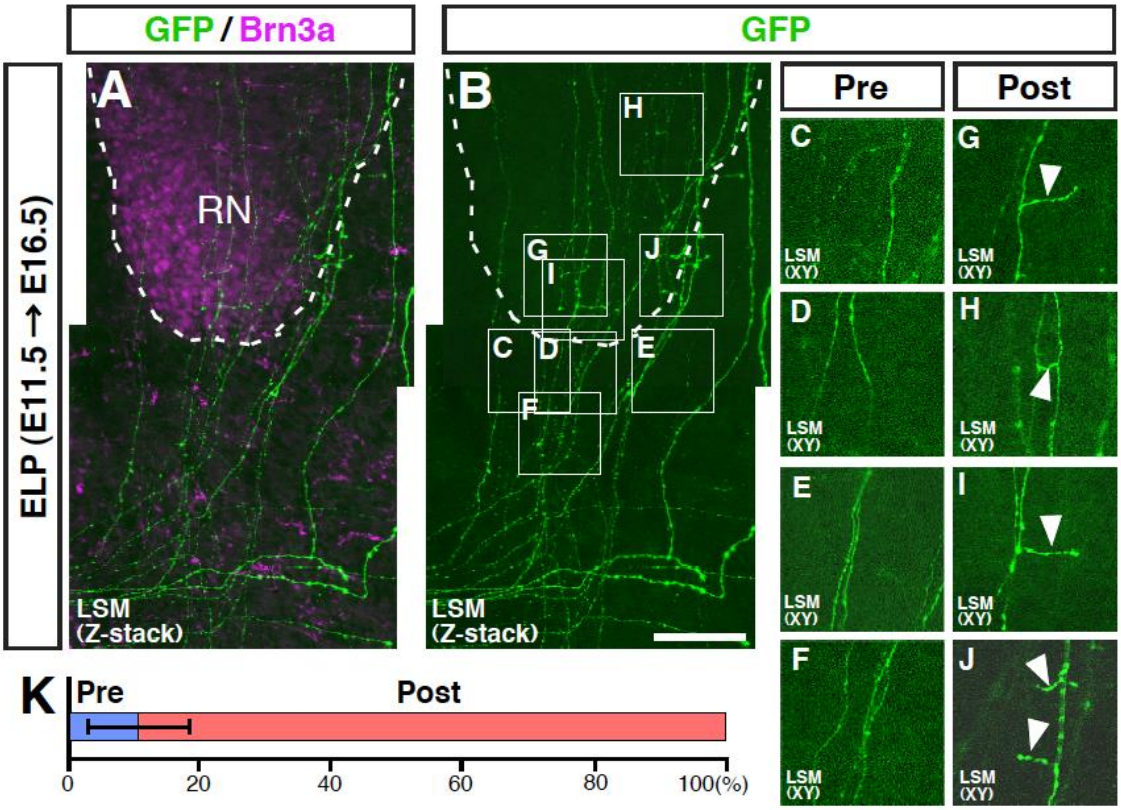
GFP / Brn3a
GFP
ELP (E11.5 → E16.5)
A
RN
LSM
(Z-stack)
B
H
G
I
J
C
D
E
F
LSM
(Z-stack)
Pre
Post
C
G
D
H
E
I
F
J
LSM
(XY)
K
Pre
Post
0
20
40
60
80
100(%)

Figure 6. Spatially restricted generation of interstitial branches.

(A, B) Photomontage of *z*-stack images of LSM optical sections (5 μm thickness) at E16.5, showing the trajectory of post-crossing GFP-labeled DCN axons after sharp rostral turn. Dashed line delineates the border of the RN. (C-F) Higher-magnification images of white boxes in B, respectively, but showing an *xy*-plane of LSM image. Representative images of axonal segments before entering the RN are shown. (G-J) High-power views of white boxes in B, respectively, but showing an *xy*-plane of LSM image. Representative images of axonal segments within the RN are displayed. Note that only the axonal segments within the RN possess interstitial branches (arrowheads). (K) Histogram showing the ratio of axons bearing the first interstitial branch at location before entering the RN (referred to as "Pre") to those at location only within the RN (referred to as "Post"). Rostral is to the top and medial (ventral) is to the left. Error bar indicates s.e.m. (*n*=4 embryos). LSM, laser scanning microscopy; RN, red nucleus. Scale bar, 100 μm in (A, B), 50 μm in (C-J).

Figure 7

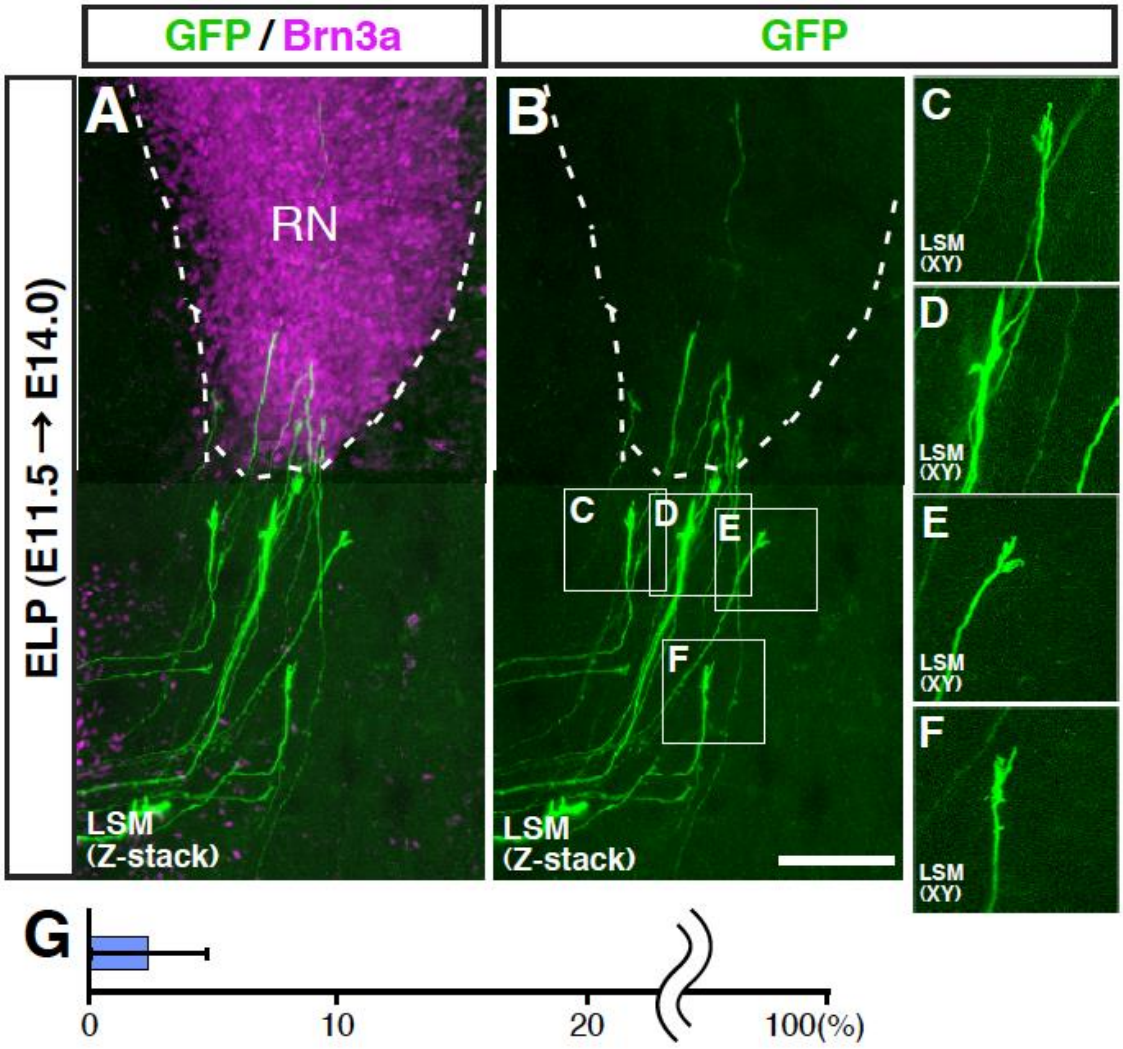
GFP / Brn3a
GFP
ELP (E11.5 → E14.0)
A
RN
LSM
(Z-stack)
B
C
D
E
F
LSM
(Z-stack)
C
LSM
(XY)
D
LSM
(XY)
E
LSM
(XY)
F
LSM
(XY)
G
0
10
20
100(%)

Figure 7. DCN axons rarely form interstitial branches prior to entering the RN.

(A, B) Photomontage of *z*-stack images of LSM optical sections (5 μm thickness) at E14, including the entire trajectory of post-crossing GFP-labeled DCN axons after sharp rostral turn. Dashed line denotes the border of the RN identified by Brn3a immunohistochemistry. (C-F) Higher-magnification views of white boxes in B, respectively, but showing an *xy*-plane of LSM image. Representative images of the shaft of DCN axons including the tip are shown. Most of the primary growth cones of DCN axons have not yet reached the RN. (G) Histogram showing the ratio of DCN axons having branches before the axonal growth cones reach the RN (*n*=5 embryos). Majority of DCN axons rarely give off interstitial branches before the primary growth cones arrive at the RN. Rostral is to the top and medial (ventral) is to the left. Error bar indicates s.e.m. LSM, laser scanning microscopy; RN, red nucleus. Scale bar, 100 μm in (A, B), 50 μm in (C-F).

Midline crossing is not required for subsequent targeting

Upon midline crossing, commissural axons acquire responsiveness to guidance cues to which they have not been sensitive before crossing (Dickson and Zou, 2010; Nawabi and Castellani, 2011). This prompted us to test whether midline crossing itself is required for subsequent targeting by DCN axons. For this, we took advantage of the fact that commissural axons including DCN axons fail to cross the floor plate in *Robo3* knockout mice (Marillat et al., 2004; Sabatier et al., 2004; Tamada et al., 2008). In this study, to prevent midline crossing, we performed *Robo3* knockdown using in vivo electroporation of *Robo3*-specific siRNA (Chen et al., 2008; Inamata and Shirasaki, 2014) (Fig. 8A). Consistent with the previous report (Tamada et al., 2008), we found that midline crossing by DCN axons was strongly inhibited by *Robo3* knockdown (Fig. 8B,D). In addition, these axons still turned to grow rostrally on the ipsilateral side (Fig. 8B,D). We found that, although the ipsilaterally growing DCN axons initially formed few interstitial branches within the RN (Fig. 8C,F), after a delay, these axons started forming interstitial branches from the portion of the axon shaft within the RN (Fig. 8E,F). These results therefore indicate that midline crossing per se is not required for subsequent targeting by DCN axons, and further suggest that DCN axons develop an intrinsic program for target recognition irrespective of midline crossing.

Figure 8

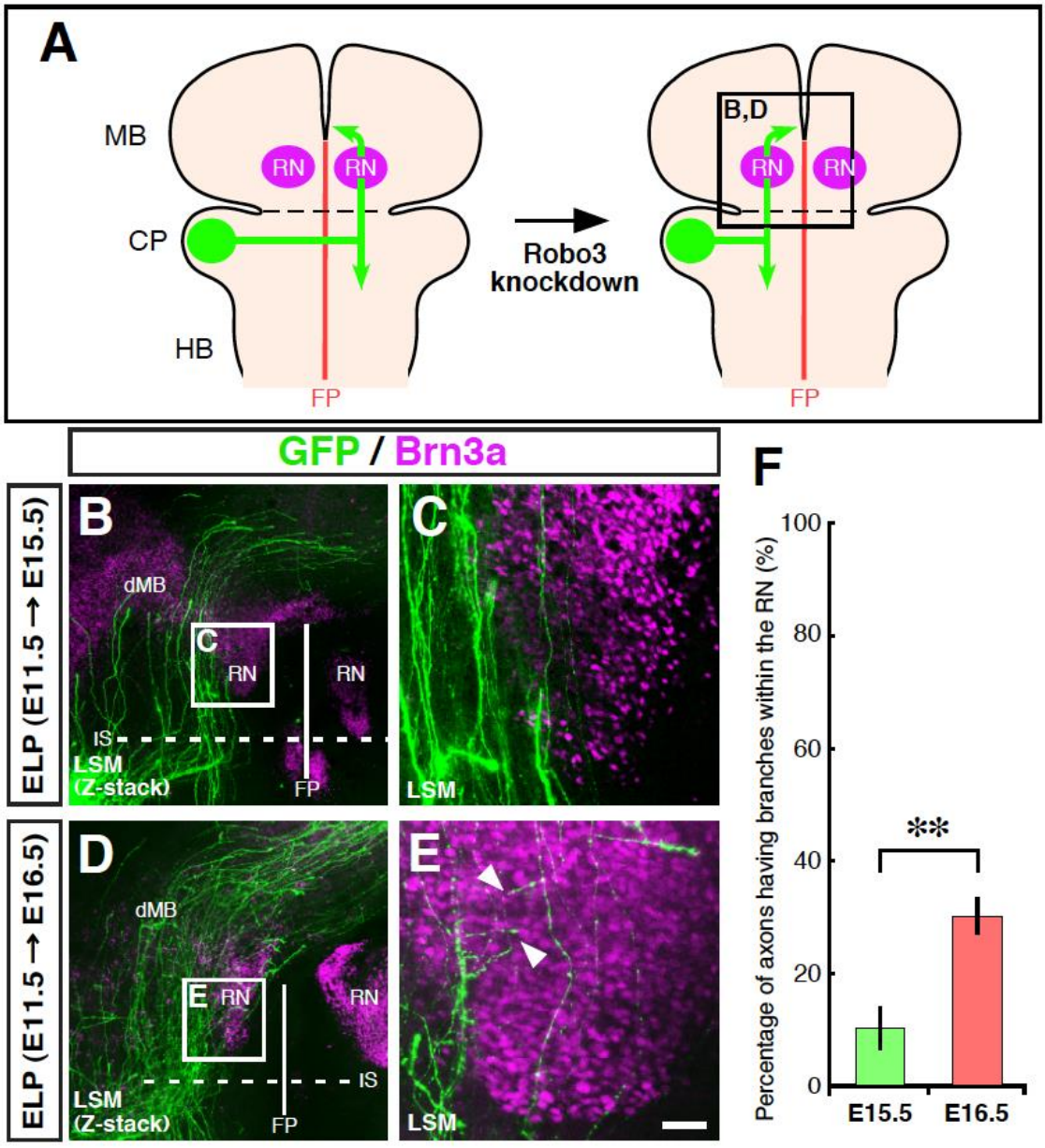
A
MB
CP
HB
RN
RN
FP
Robo3
knockdown
B,D
RN
RN
FP
GFP / Brn3a
ELP (E11.5 → E15.5)
ELP (E11.5 → E16.5)
B
dMB
C
RN
RN
IS
LSM
(Z-stack)
FP
C
LSM
D
dMB
E
RN
RN
IS
LSM
(Z-stack)
FP
E
LSM
F
Percentage of axons having branches within the RN (%)
100
80
60
40
20
0
**
E15.5
E16.5

Figure 8. Midline crossing is not required for subsequent targeting.

(A) Schematic showing an experimental design for the analysis of DCN axon behavior within the RN in *Robo3* knockdown embryos. Loss of *Robo3* function results in failure of midline crossing by DCN axons. These axons instead grow ipsilaterally (see also Tamada et al., 2008). The Brn3a expression in the ventral midbrain region marks the location of the RN. (B, C) Behavior of GFP-labeled DCN axons in *Robo3* knockdown embryos at E15.5. DCN axons that have been prevented from midline crossing grow rostrally away from the midline on the ipsilateral side. Note that DCN axons that have entered the RN overshoot the RN. (B) Higher-magnified image of black rectangle in A, showing a *z*-stack image of 18 optical sections (10 μm thickness) obtained by confocal LSM. (C) High-power view of white box in B, but showing an *xy*-plane of LSM image within and around the RN. DCN axons give off few interstitial branches within the ipsilateral RN at this stage. (D, E) Behavior of DCN axons in *Robo3* knockdown embryos at E16.5. (D) Higher-magnified image of black rectangle in A, showing a *z*-stack image of 21 optical sections (10 μm thickness) captured by confocal LSM. (E) High-power view of white box in D, but showing a *z*-stack LSM image of 6 optical sections (5 μm thickness) in order to trace several representative branches (arrowheads) completely within the RN. At E16.5, many DCN axons develop interstitial branches from the portion of the axon shaft within the RN. (F) Quantification of the ratio of GFP-labeled DCN axons that have interstitial branches within the ipsilateral RN in *Robo3* knockdown embryos at E15.5 (green, n=4 embryos) and at E16.5 (red, n=5 embryos). Error bars indicate s.e.m. Statistical significance was determined by

Student's *t*-test (**P<0.01). Notably, after a delay, DCN axons that have entered the ipsilateral RN initiate forming interstitial branches within the RN. Rostral is to the top (A-E). Medial (ventral) is to the right (C, E). CP, cerebellar plate; dMB, dorsal midbrain; FP, floor plate; HB, hindbrain; IS, isthmus; LSM, laser scanning microscopy; MB, midbrain; RN, red nucleus. Scale bar, 200 μm in (B, D), 50 μm in (C, E).

DISCUSSION

In this study, in order to examine how DCN axons recognize their targets, we analyzed in detail the behavior of genetically identified DCN axons during the time when these axons project to the RN. We found that, when DCN axons initially entered the RN at its caudal end, these axons continued to grow rostrally within the RN without showing noticeable morphological signs of axon branching. Intriguingly, after a delay, DCN axons started forming interstitial branches from the portion of the axon shaft selectively within the RN. Furthermore, these axons still formed interstitial branches within the RN even in the absence of midline crossing. These results therefore suggest that the mechanism of RN recognition by DCN axons involves a delayed interstitial branching (Fig. 9), and that midline crossing per se is not required for the process of target recognition in this system.

The Process of RN Recognition by DCN axons

Tsukahara and his colleagues first demonstrated electrophysiologically that the RN is a direct synaptic target of DCN neurons (Tsukahara et al., 1967). Electrophysiological and anatomical studies later suggested that DCN neurons project to a wide array of targets in the brain and spinal cord (Chan-Palay, 1977). In particular, Shinoda et al. (1988) have clearly shown at the single-axon level that most of the DCN neurons projecting to the thalamus give off collateral branches within the RN from their axon shafts. However, it remained unknown whether the collateral branches are formed by bifurcation of the primary axonal growth cone or by interstitial branching from the axon

shaft behind the terminal growth cone. In the present study, we show that collateral branches extend interstitially from the shaft of DCN axons behind the primary axonal growth cone. Moreover, we show that the interstitial branching occurs from the portion of the axon shaft selectively within the RN. These observations suggest that the process of RN recognition by DCN axons is a property of the axon shaft rather than the leading growth cone. Importantly, this is quite reminiscent of a prominent example of collateralization of layer 5 corticospinal neurons in the mammalian neocortex (O'Leary et al., 1990). In this system, corticospinal axons initially bypass their subcortical synaptic targets such as the basilar pons, but after a delay, they form interstitial branches from the portion of the axon shaft overlying the pons, which then arborize once they have entered the pons (O'Leary and Terashima, 1988; Bastmeyer and O'Leary, 1996). Thus, it is now becoming increasingly apparent that the process of target recognition commonly observed in many classes of long-projecting neurons in the vertebrate CNS involves axon branches that extend interstitially from the selective segment of the axon shaft located most proximal to their synaptic targets (see also Kalil and Dent, 2014, and references therein).

Correspondence of labeled DCN axons to those in previous studies

It is known that DCN axon projection to the RN in mammals is topographically organized (Paxinos, 2004). In this study in mice, the rostrocaudal preference of branch formation by DCN axons was not observed (Fig.5C). This result may be due to the methods employed in this study, since DCN axon labeling by Atoh1 enhancer

technically visualized both the interposed and the lateral nuclei simultaneously. Previous studies also reported that DCN axons make synaptic connection with the RN, the thalamus, or both of them in adult (Tsukahara et al., 1967; Chan-Palay, 1977). In this study, the variation of the axonal projection patterns that reflects those circuitries was not evident. Considering that the circuit formation by DCN axons is still under development even at the late embryonic stages, there is a possibility that the variation of the projection pattern may become prominent at later embryonic or at postnatal stages in rodents. Further detailed considerations will be needed to obtain any findings related to these issues.

Midline crossing and subsequent targeting

It is known that axon responsiveness to guidance cues changes with prior experience, affecting subsequent behaviors of growing axons (Snow and Letourneau, 1992; Shirasaki et al., 1998; Cai et al., 1999; Höpker et al., 1999; Diefenbach et al., 2000; Zou et al,. 2000; Ming et al., 2002; Charoy et al., 2012). During development, when growing axons navigate long distances to reach their final targets, intermediate targets help them achieve this challenging task. In general, after growing past those intermediate targets, axons change their behaviors to adopt a new trajectory on the other side. Currently, the best-characterized intermediate target is the floor plate that occupies the ventral midline of the neural tube (Dickson and Zou, 2010). Importantly, it has been shown that commissural axons dramatically change responsiveness to various guidance cues upon crossing the floor plate (Shirasaki et al., 1998; Zou et al., 2000; Nawabi and Castellani,

2011). In addition, recent studies have clearly shown that, when crossing the floor plate, commissural axons receive signals that induce long-term modification of their behaviors on the contralateral side (Kuwako et al., 2010; Charoy et al., 2012; Colak et al., 2013). Indeed, after these axons have once crossed the floor plate, they abruptly change their growth direction from the circumferential to the longitudinal axis and never re-enter the floor plate. Because target recognition by these axons occurs only after crossing the floor plate (or midline crossing), this has raised an interesting question of whether midline crossing itself is required for reception of target-derived cues normally received by post-crossing axons. However, in the present study, we show that DCN axons are still capable of forming interstitial branches within the RN even in the absence of midline crossing. Consistent with this observation, olivocerebellar axons and commissural axons from the ventral cochlear nucleus, even when midline crossing is prevented, can still grow toward and connect to their appropriate final targets – albeit on the incorrect ipsilateral side of the brain (Kuwako et al., 2010; Renier et al., 2010). These studies, together with our current data, therefore suggest that commissural axons possess an intrinsic ability to respond to the target-derived cues, and that midline-crossing experience is not strictly required for subsequent targeting in the bilaterally symmetrical vertebrate CNS.

Mechanism of delayed interstitial branching by DCN axons

The primary axonal growth cones in the vertebrate CNS typically do not enter their target regions and initially bypass them, followed by extension of interstitial branches

into their eventual terminal sites, as exemplified by corticopontine projection described above. On the other hand, the primary growth cone of DCN axons enters the RN from the beginning and, after a delay, these axons start forming interstitial branches from the portion of the axon shaft selectively within the RN (Fig. 9). This implies that short-range locally acting cues, rather than long-range diffusible ones (Heffner et al., 1990; Sato et al., 1994), are involved in the formation of interstitial branches from the shaft of DCN axons. Notably, among such kind of molecules with axon branch-inducing activity, Slit2 might be a prime candidate (Wang et al., 1999), since the RN expresses *slit2* at the stage of interstitial branching by DCN axons and DCN axons express *robo1* at around this stage (Marillat et al., 2002). On the other hand, Slit has been suggested to act as a repellent for DCN axons just after these axons cross the floor plate (Tamada et al., 2008). Therefore, in order for Slit to function as a branch-inducing attractant within the RN, it is necessary to assume that DCN axons intrinsically change responsiveness to Slit from repulsion to attraction by the time when DCN axons initiate interstitial branching. In this context, it should be noted that dissociated commissural

Figure 9

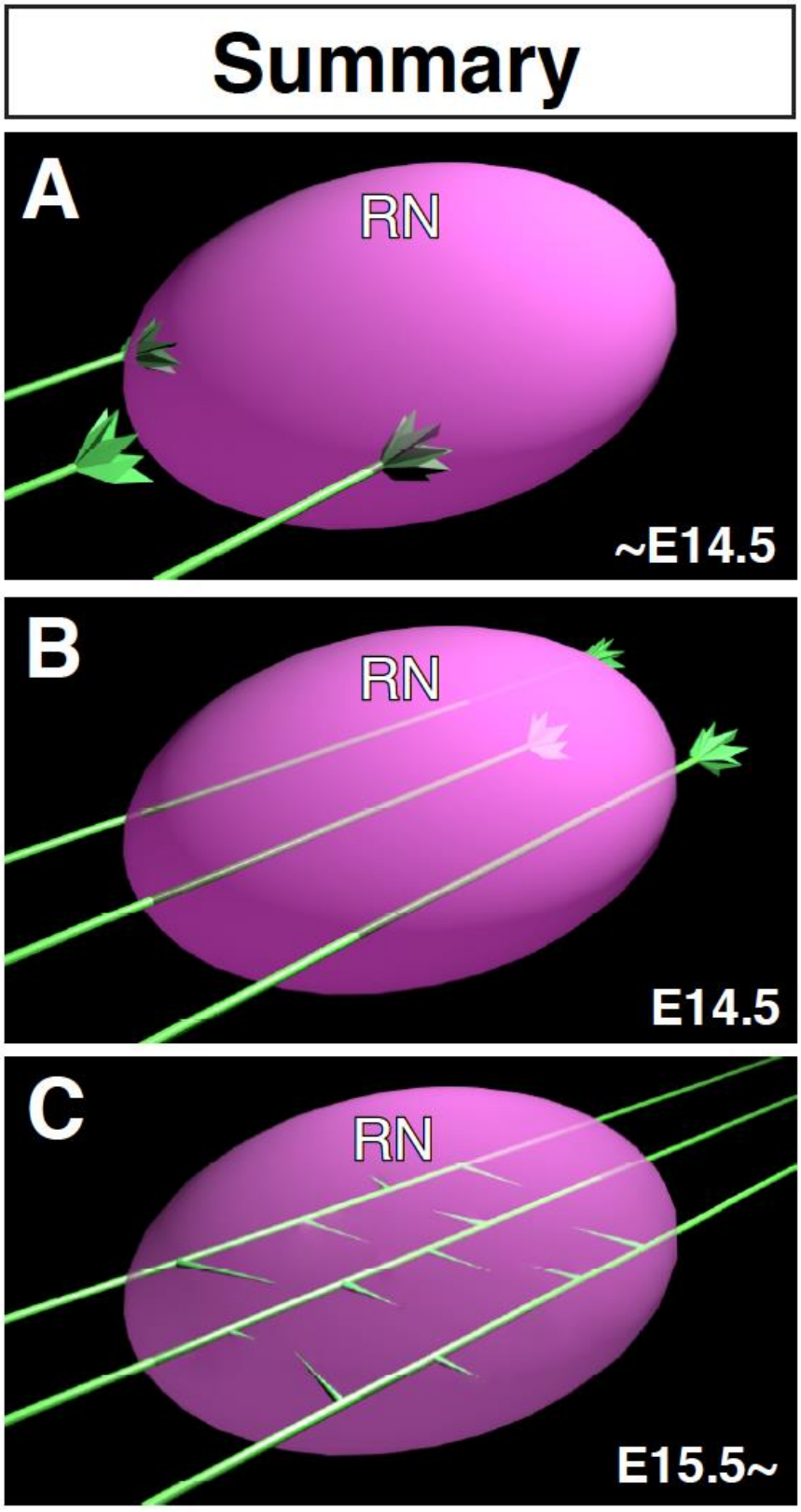

Figure 9. Summary diagram illustrating the present findings.

Development of interstitial branches by DCN axons (green) within the RN (purple) is described. (A) Post-crossing DCN axons turn to grow rostrally toward the RN without axon branching. Some of the DCN axons start entering the RN at its caudal end at E14. (B) At around E14.5, the majority of DCN axons enter the RN and continue to grow rostrally through the RN without showing noticeable morphological signs of axon branching within the RN. (C) At E15.5 and older, DCN axons develop interstitial branches from the portion of the axon shaft selectively within the RN. Moreover, even in the absence of midline crossing, DCN axons can still form interstitial branches within the RN on the ipsilateral side. These findings therefore suggest that the mechanism of RN recognition by DCN axons involves a delayed interstitial branching, and that these axons possess an intrinsic ability to respond to the target-derived cues irrespective of midline crossing.

neurons in vitro have recently been shown to switch their response to Shh from attraction to repulsion after an extended time in culture (Yam et al., 2012). Thus, it is tempting to speculate that a similar cell-intrinsic temporal switch in responsiveness to Slit is in some way involved in the delayed interstitial branching by DCN axons within the RN. Future studies will aim to address this intriguing possibility.

REFERENCES

Altman J, Bayer SA. 1978. Prenatal development of the cerebellar system in the rat. I. Cytogenesis and histogenesis of the deep nuclei and the cortex of the cerebellum. J Comp Neurol 179:23-48.

Altman J, Bayer SA. 1997. The Development of the Cerebellar System: In Relation to Its Evolution, Structure, and Functions (Boca Raton, FL: CRC Press).

Badea TC, Wang Y, Nathans J. 2003. A noninvasive genetic/pharmacologic strategy for visualizing cell morphology and clonal relationships in the mouse. J Neurosci 23:2314-2322.

Bastmeyer M, O'Leary DD. 1996. Dynamics of target recognition by interstitial axon branching along developing cortical axons. J Neurosci 16:1450-1459.

Batini C, Compoint C, Buissseret-Delmas C, Daniel H, Guegan M. 1992. Cerebellar nuclei and the nucleocortical projections in the rat: retrograde tracing coupled to GABA and glutamate immunohistochemistry. J Comp Neurol 315:74-84.

Bengtsson F, Hesslow G. 2006. Cerebellar control of the inferior olive. Cerebellum 5:7-14.

Bourikas D, Pekarik V, Baeriswyl T, Grunditz A, Sadhu R, Nardó M, Stoeckli ET. 2005. Sonic hedgehog guides commissural axons along the longitudinal axis of the spinal cord. Nat Neurosci 8:297-304.

Brodal P. 1992. The Central Nervous System (New York: Oxford University Press), 262-282.

Cai D, Shen Y, De Bellard M, Tang S, Filbin MT. 1999. Prior exposure to neurotrophins blocks inhibition of axonal regeneration by MAG and myelin via a

cAMP-dependent mechanis. Neuron 22:89-101.

Chan-Palay V. 1977. Cerebellar Dentate Nucleus: Organization, Cytology and Transmitters. (New York: Springer-Verlag).

Charoy C, Nawabi H, Reynaud F, Derrington E, Bozon M, Wright K, Falk J, Helmbacher F, Kindbeiter K, Castellani V. 2012. gdnf activates midline repulsion by Semaphorin3B via NCAM during commissural axon guidance. Neuron 75:1051-1066.

Chédotal A. 2014. Development and plasticity of commissural circuits: from locomotion to brain repair. Trends Neurosci 37:551-562.

Chen Z, Gore BB, Long H, Ma L, Tessier-Lavigne M. 2008. Alternative splicing of the Robo3 axon guidance receptor governs the midline switch from attraction to repulsion. Neuron 58:325-332.

Cohen-Cory S, Fraser SE. 1995. Effects of brain-derived neurotrophic factor on optic axon branching and remodelling in vivo. Nature 378:192-196.

Colak D, Ji SJ, Porse BT, Jaffrey SR. 2013. Regulation of axon guidance by compartmentalized nonsense-mediated mRNA decay. Cell 153:1252-1265.

Dickson BJ. 2002. Molecular mechanisms of axon guidance. Science 298:1959-1964.

Dickson BJ, Zou Y. 2010. Navigating intermediate targets: the nervous system midline. Cold Spring Harb Perspect Biol 2:a002055.

Diefenbach TJ, Guthrie PB, Kater SB. 2000. Stimulus history alters behavioral responses of neuronal growth cones. J Neurosci 20:1484-1494.

Fredette BJ, Mugnaini E. 1991. The GABAergic cerebello-olivary projection in the rat. Anat Embryol (Berl) 184:225-243.

Heffner CD, Lumsden AG, O'Leary DD. 1990. Target control of collateral extension and directional axon growth in the mammalian brain. Science 247:217-220.

Helms AW, Abney AL, Ben-Arie N, Zoghbi HY, Johnson JE. 2000. Autoregulation and multiple enhancers control Math1 expression in the developing nervous system. Development 127:1185-1196.

Höpker VH, Shewan D, Tessier-Lavigne M, Poo M, Holt C. 1999. Growth-cone attraction to netrin-1 is converted to repulsion by laminin-1. Nature 401:69-73.

Hoshino M, Nakamura S, Mori K, Kawauchi T, Terao M, Nishimura YV, Fukuda A, Fuse T, Matsuo N, Sone M, Watanabe M, Bito H, Terashima T, Wright CV, Kawaguchi Y, Nakao K, Nabeshima Y. 2005. Ptf1a, a bHLH transcriptional gene, defines GABAergic neuronal fates in cerebellum. Neuron 47:201-213.

Inamata Y, Shirasaki R. 2014. Dbx1 triggers crucial molecular programs required for midline crossing by midbrain commissural axons. Development 141:1260-1271.

Ito M. 1984. The Cerebellum and Neural Control (New York: Raven Press).

Jefferis GS, Livet J. 2012. Sparse and combinatorial neuron labelling. Curr Opin Neurobiol 22:101-110.

Jiang MC, Alheid GF, Nunzi MG, Houk JC. 2002. Cerebellar input to magnocellular neurons in the red nucleus of the mouse: synaptic analysis in horizontal brain slices incorporating cerebello-rubral pathways. Neuroscience 110:105-121.

Kalil K, Dent EW. 2014. Branch management: mechanisms of axon branching in the developing vertebrate CNS. Nat Rev Neurosci 15:7-18.

Kennedy TE, Serafini T, de la Torre JR, Tessier-Lavigne M. 1994. Netrins are diffusible chemotropic factors for commissural axons in the embryonic spinal cord. Cell 78:425-435.

Kolodkin AL, Tessier-Lavigne M. 2011. Mechanisms and molecules of neuronal wiring: a primer. Cold Spring Harb Perspect Biol. 3:a001727.

Kuwako K, Kakumoto K, Imai T, Igarashi M, Hamakubo T, Sakakibara S, Tessier-Lavigne M, Okano HJ, Okano H. 2010. Neural RNA-binding protein Musashi1 controls midline crossing of precerebellar neurons through posttranscriptional regulation of Robo3/Rig-1 expression. Neuron 67:407-421.

Lyuksyutova AI, Lu CC, Milanesio N, King LA, Guo N, Wang Y, Nathans J, Tessier-Lavigne M, Zou Y. 2003. Anterior-posterior guidance of commissural axons by Wnt-frizzled signaling. Science 302:1984-1988.

Machold R, Fishell G. 2005. Math1 is expressed in temporally discrete pools of cerebellar rhombic-lip neural progenitors. Neuron 48:17-24.

Marillat V, Cases O, Nguyen-Ba-Charvet KT, Tessier-Lavigne M, Sotelo C, Chédotal A. 2002. Spatiotemporal expression patterns of slit and robo genes in the rat brain. J Comp Neurol 442:130-155.

Marillat V, Sabatier C, Failli V, Matsunaga E, Sotelo C, Tessier-Lavigne M, Chédotal A. 2004. The slit receptor Rig-1/Robo3 controls midline crossing by hindbrain precerebellar neurons and axons. Neuron 43:69-79.

McEvilly RJ, Erkman L, Luo L, Sawchenko PE, Ryan AF, Rosenfeld MG. 1996. Requirement for Brn-3.0 in differentiation and survival of sensory and motor neurons. Nature 384:574-577.

Ming GL, Wong ST, Henley J, Yuan XB, Song HJ, Spitzer NC, Poo MM. 2002. Adaptation in the chemotactic guidance of nerve growth cones. Nature 417:411-418.

Miyoshi G, Fishell G. 2006. Directing neuron-specific transgene expression in the mouse CNS. Curr Opin Neurobiol 16:577-584.

Nakagawa Y, O'Leary DD. 2001. Combinatorial expression patterns of LIM-homeodomain and other regulatory genes parcellate developing thalamus. J Neurosci 21:2711-2725.

Nakamura S, Watanabe S, Ohtsuka M, Maehara T, Ishihara M, Yokomine T, Sato M. 2008. Cre-loxP system as a versatile tool for conferring increased levels of tissue-specific gene expression from a weak promoter. Mol Reprod Dev 75:1085-1093.

Nakatani T, Minaki Y, Kumai M, Ono Y. 2007. Helt determines GABAergic over glutamatergic neuronal fate by repressing Ngn genes in the developing mesencephalon. Development 134:2783-2793.

Nawabi H, Castellani V. 2011. Axonal commissures in the central nervous system: how to cross the midline? Cell Mol Life Sci 68:2539-2553.

Niwa H, Yamamura K, Miyazaki J. 1991. Efficient selection for high-expression transfectants with a novel eukaryotic vector. Gene 108:193-199.

O'Leary DD, Terashima T. 1988. Cortical axons branch to multiple subcortical targets by interstitial axon budding: implications for target recognition and "waiting periods". Neuron 1:901-910.

O'Leary DD, Bicknese AR, De Carlos JA, Heffner CD, Koester SE, Kutka LJ, Terashima T. 1990. Target selection by cortical axons: alternative mechanisms to establish axonal connections in the developing brain. Cold Spring Harb Symp Quant Biol 55:453-468.

Ono Y, Nakatani T, Minaki Y, Kumai M. 2010. The basic helix-loop-helix transcription factor Nato3 controls neurogenic activity in mesencephalic floor plate cells. Development 137:1897-1906.

Paxinos G. 2004. The Rat Nervous System. (3rd ed) (New York: Elsevier Academic

Press).

Pierce ET. 1975. Histogenesis of the deep cerebellar nuclei in the mouse: an autoradiographic study. Brain Res 95:503-518.

Prakash N, Puelles E, Freude K, Trumbach D, Omodei D, Di Salvio M, Sussel L, Ericson J, Sander M, Simeone A, Wurst W. 2009. Nkx6-1 controls the identity and fate of red nucleus and oculomotor neurons in the mouse midbrain. Development 136:2545-2555.

Renier N, Schonewille M, Giraudet F, Badura A, Tessier-Lavigne M, Avan P, De Zeeuw CI, Chédotal A. 2010. Genetic dissection of the function of hindbrain axonal commissures. PLoS Biol 8:e1000325.

Rotolo T, Smallwood PM, Williams J, Nathans J. 2008. Genetically-directed, cell type-specific sparse labeling for the analysis of neuronal morphology. PLoS One 3:e4099.

Saba R, Nakatsuji N, Saito T. 2003. Mammalian BarH1 confers commissural neuron identity on dorsal cells in the spinal cord. J Neurosci 23:1987-1991.

Sabatier C, Plump AS, Le M, Brose K, Tamada A, Murakami F, Lee EY, Tessier-Lavigne M. 2004. The divergent Robo family protein rig-1/Robo3 is a negative regulator of slit responsiveness required for midline crossing by commissural axons. Cell 117:157-169.

Saito T. 2006. In vivo electroporation in the embryonic mouse central nervous system. Nat Protoc 1:1552-1558.

Sato M, Yasuoka Y, Kodama H, Watanabe T, Miyazaki J, Kimura M. 2000. New approach to cell lineage analysis in mammals using the Cre-loxP system. Mol Reprod Dev 56:34-44.

Sato M, Lopez-Mascaraque L, Heffner CD, O'Leary DD. 1994. Action of a diffusible target-derived chemoattractant on cortical axon branch induction and directed growth. Neuron 13:791-803.

Schneider CA, Rasband WS, Eliceiri KW. 2012. NIH Image to ImageJ: 25 years of image analysis. Nat Methods 9:671-675.

Schwarz C, Schmitz Y. 1997. Projection from the cerebellar lateral nucleus to precerebellar nuclei in the mossy fiber pathway is glutamatergic: a study combining anterograde tracing with immunogold labeling in the rat. J Comp Neurol 381:320-334.

Serafini T, Kennedy TE, Galko MJ, Mirzayan C, Jessell TM, Tessier-Lavigne M. 1994. The netrins define a family of axon outgrowth-promoting proteins homologous to C. elegans UNC-6. Cell 78:409-424.

Shimogori T, Ogawa M. 2008. Gene application with in utero electroporation in mouse embryonic brain. Dev Growth Differ 50:499-506.

Shinoda Y, Futami T, Mitoma H, Yokota J. 1988. Morphology of single neurones in the cerebello-rubrospinal system. Behav Brain Res 28:59-64.

Shirasaki R, Katsumata R, Murakami F. 1998. Change in chemoattractant responsiveness of developing axons at an intermediate target. Science 279:105-107.

Shirasaki R, Lewcock JW, Lettieri K, Pfaff SL. 2006. FGF as a target-derived chemoattractant for developing motor axons genetically programmed by the LIM code. Neuron 50:841-853.

Shirasaki R, Mirzayan C, Tessier-Lavigne M, Murakami F. 1996. Guidance of circumferentially growing axons by netrin-dependent and -independent floor plate chemotropism in the vertebrate brain. Neuron 17:1079-1088.

Shirasaki R, Murakami F. 2001. Crossing the floor plate triggers sharp turning of

commissural axons. Dev Biol 236:99-108.

Shirasaki R, Tamada A, Katsumata R, Murakami F. 1995. Guidance of cerebellofugal axons in the rat embryo: directed growth toward the floor plate and subsequent elongation along the longitudinal axis. Neuron 14:961-972.

Snow DM, Letourneau PC. 1992. Neurite outgrowth on a step gradient of chondroitin sulfate proteoglycan (CS-PG). J Neurobiol 23:322-336.

Su HL, Muguruma K, Matsuo-Takasaki M, Kengaku M, Watanabe K, Sasai Y. 2006. Generation of cerebellar neuron precursors from embryonic stem cells. Dev Biol 290:287-296.

Tabata H, Nakajima K. 2001. Efficient in utero gene transfer system to the developing mouse brain using electroporation: visualization of neuronal migration in the developing cortex. Neuroscience 103:865-872.

Tamada A, Kumada T, Zhu Y, Matsumoto T, Hatanaka Y, Muguruma K, Chen Z, Tanabe Y, Torigoe M, Yamauchi K, Oyama H, Nishida K, Murakami F. 2008. Crucial roles of Robo proteins in midline crossing of cerebellofugal axons and lack of their up-regulation after midline crossing. Neural Dev 3:29.

Tessier-Lavigne M, Placzek M, Lumsden AG, Dodd J, Jessell TM. 1988. Chemotropic guidance of developing axons in the mammalian central nervous system. Nature 336:775-778.

Toyama K, Tsukahara N, Kosaka K, Matsunami K. 1970. Synaptic excitation of red nucleus neurones by fibres from interpositus nucleus. Exp Brain Res 11:187-198.

Tsukahara N, Toyama K, Kosaka K. 1967. Electrical activity of red nucleus neurones investigated with intracellular microelectrodes. Exp Brain Res 4:18-33.

Wang KH, Brose K, Arnott D, Kidd T, Goodman CS, Henzel W, Tessier-Lavigne M.

1999. Biochemical purification of a mammalian slit protein as a positive regulator of sensory axon elongation and branching. Cell 96:771-784.

Wang VY, Rose MF, Zoghbi HY. 2005. Math1 expression redefines the rhombic lip derivatives and reveals novel lineages within the brainstem and cerebellum. Neuron 48:31-43.

Xiang M, Gan L, Zhou L, Klein WH, Nathans J. 1996. Targeted deletion of the mouse POU domain gene Brn-3a causes selective loss of neurons in the brainstem and trigeminal ganglion, uncoordinated limb movement, and impaired suckling. Proc Natl Acad Sci U S A 93:11950-11955.

Yam PT, Kent CB, Morin S, Farmer WT, Alchini R, Lepelletier L, Colman DR, Tessier-Lavigne M, Fournier AE, Charron F. 2012. 14-3-3 proteins regulate a cell-intrinsic switch from sonic hedgehog-mediated commissural axon attraction to repulsion after midline crossing. Neuron 76:735-749.

Young P, Feng G. 2004. Labeling neurons in vivo for morphological and functional studies. Curr Opin Neurobiol 14:642-646.

Zou Y, Stoeckli E, Chen H, Tessier-Lavigne M. 2000. Squeezing axons out of the gray matter: a role for slit and semaphorin proteins from midline and ventral spinal cord. Cell 102:363-375.

BIBLIOGRAPHY

(1) Original Article

Hara S, Kaneyama T, Inamata Y, Onodera R, and Shirasaki R (2016).
Interstitial Branch Formation within the Red Nucleus by Deep Cerebellar Nuclei-Derived Commissural Axons during Target Recognition.
The Journal of Comparative Neuroscience 524, 999-1014.

(2) Japanese Scientific Meeting (Poster Presentation)

Hara S, Onodera R, Inamata Y, and Shirasaki R (2011).
Target recognition by commissural neurons genetically defined by Atoh1 in the mouse cerebellum.
The 34th Annual Meeting of the Japan Neuroscience Society, Yokohama Japan.

Hara S, Onodera R, Inamata Y,, and Shirasaki R (2012).
Target recognition and interstitial axon branching by DI1-type commissural neurons in the mouse cerebellum.
The 35th Annual Meeting of the Japan Neuroscience Society, Nagoya, Japan.

ACKNOWLEDGMENTS

I would like to express my greatest appreciation to my supervisor Dr. Ryuichi Shirasaki for providing me with this precious opportunity in my Ph.D course. His continuing support, insightful comments, and constant encouragements were invaluable during the course of my study. I am deeply grateful to Dr. Nobuhiko Yamamoto for his persistent encouragements and helpful advice on this thesis from the beginning of my work. I want to thank Dr. Takeshi Yagi, Dr. Shigeru Kitazawa, and Dr. Yasushi Kobayashi for the helpful advice and comments on this thesis. I also thank Dr. Yoshiki Sasai for providing us with Atoh1 enhancer element, Dr. Masahiro Sato for the original Cre/LoxP system, and Dr. Jun-ichi Miyazaki for pCAGGS vector. I received generous support from members of the Shirasaki group for their enormous help and comments in my experiments. Especially, I thank Dr. Yasuyuki Inamata for generating the Atoh1 enhancer-Cre and Atoh1 enhancer-ZsGreen vectors as well as pCAGGS-LoxP-CAT-LoxP-AcGFP1 vector, Ryota Onodera for sharing the theme of this research, and Takeshi Kaneyama for participating in some of the critical experiments and data analyses. I also thank Ryosuke Otobe for technical assistance. I offer my special thanks to the members of the Yamamoto lab for their encouragements. Finally, I would like to show my gratitude to my family for their continuous support and warm encouragements.